EXPANDED MIXED MULTISCALE FINITE ELEMENT METHODS AND THEIR APPLICATIONS FOR FLOWS IN POROUS MEDIA *

L. JIANG†, D. COPELAND‡, AND J. D. MOULTON§

Abstract. We develop a family of expanded mixed Multiscale Finite Element Methods (MsFEMs) and their hybridizations for second-order elliptic equations. This formulation expands the standard mixed Multiscale Finite Element formulation in the sense that four unknowns (hybrid formulation) are solved simultaneously: pressure, gradient of pressure, velocity, and Lagrange multipliers. We use multiscale basis functions for both the velocity and the gradient of pressure. In the expanded mixed MsFEM framework, we consider both separable and non-separable spatial scales. Specifically, we analyze the methods in three categories: periodic separable scales, $G-$convergent separable scales, and a continuum of scales. When there is no scale separation, using some global information can significantly improve the accuracy of the expanded mixed MsFEMs. We present a rigorous convergence analysis of these methods that includes both conforming and nonconforming formulations. Numerical results are presented for various multiscale models of flow in porous media with shale barriers that illustrate the efficacy of the proposed family of expanded mixed MsFEMs.

Key words. expanded mixed multiscale finite element methods, non-separable scales, hybridization, two-phase flows

AMS subject classifications. 65N99, 65N30, 34E13

1. Introduction.

There are many fundamental and practical problems involving a wide range of length scales. Typical examples include highly heterogeneous porous media and composite materials with fine micro-structures. In practice, these scales are too fine to treat with direct numerical simulation as the computational cost far exceeds the capabilities of computers for the foreseeable future. As a result, it is a significant challenge, both theoretically and numerically, to treat problems with multiple-scales effectively. A variety of numerical algorithms, varying from upscaling to multiscale methods, have been developed to capture the influence of fine-scale spatial heterogeneity on coarse-scale properties of the solution. In most upscaling methods the coarse-scale model is developed by numerically homogenizing (or averaging) the parameters of the fine-scale model, such as permeability. The form of the coarse-scale model is typically assumed to be the same as the fine-scale model. Simulations are performed using the coarse-scale model, and coarse-scale quantities of interest are readily computed. However, with this parameter upscaling, fine-scale properties of the solution can no longer be recovered. In contrast, multiscale methods carry fine-scale information throughout the simulation, and the coarse-scale equations are generally not expressed analytically, but rather formed and solved numerically.

Various numerical multiscale approaches have been developed during the past decade. A Multiscale Finite Element Method (MsFEM) was introduced in [23] and

*L. Jiang and J. D. Moulton acknowledge the fund by the Department of Energy at Los Alamos National Laboratory under contracts DE-AC52-06NA25396 and the DOE Office of Science Advanced Computing Research (ASCR) program in Applied Mathematical Sciences. D. Copeland acknowledges the support of Award No. KUS-C1-016-04, made by King Abdullah University of Science and Technology (KAUST).

†Applied Mathematics and Plasma Physics, Los Alamos National Laboratory, NM 87545 (ljiang@lanl.gov), Corresponding author.

‡Department of Mathematics, Texas A&M University, College Station, TX, 77840 (dylancopeland@gmail.com).

§Applied Mathematics and Plasma Physics, Los Alamos National Laboratory, NM 87545 (moulton@lanl.gov).

takes its origin from the pioneering work [9]. Its main idea is to incorporate fine-scale information into the finite element basis functions and capture their effect on coarse scales via finite element formulations. In many cases, the multiscale basis functions can be pre-computed and used repeatedly in subsequent computations with different source terms, boundary conditions and even slightly different coefficients. In some situations the bases can be updated adaptively. This leads to a large computational saving in upscaling multi-phase flows where the pressure equation needs to be solved many times dynamically. There are a number of other multiscale numerical methods with different approaches, such as residual free bubbles [11], the variational multiscale method [24], two-scale conservative subgrid upscaling [4] and the heterogeneous multiscale method [17]. Arbogast et al. [6] used a domain decomposition approach and variational mixed formulation to develop a multiscale mortar mixed MsFEM. Jenny et al. [25] have used a set of multiscale basis functions similar to [23] to develop a Multiscale Finite Volume Method (MsFV). A Multilevel Multiscale Method [28] was proposed in the framework of the Mimetic Finite Difference Method that efficiently evolves a hierarchy of coarse-scale models. In recent years, multiscale methods (e.g., [10, 15, 18]) have been developed to address high-contrast in multiscale coefficients.

The mixed multiscale method was first developed by Arbogast et.al. [4] as a locally conservative subgrid upscaling method, and was later analyzed and extended in [5] using a variational multiscale formulation. Chen and Hou developed a local multiscale basis equation for velocity and combined it with a mixed finite element formulation to propose a mixed MsFEM [14]. The mixed MsFEMs retain local conservation of mass and have been found to be useful for solving flow equations in heterogeneous porous media and other applications. However, in many practical situations, the permeability may be very low, and even vanish in some regions of the domain (e.g., permeability in shale). In this case its inverse is not readily available for use in the standard mixed MsFEM formulation, and hence, the direct application of these methods to practical problems may be restricted. To overcome this limitation, we propose a family of expanded mixed MsFEMs for these multiscale applications.

Expanded Mixed Finite Element Methods (MFEMs) were studied in classic finite element spaces in the past. Chen [13] developed and analyzed expanded MFEMs for second-elliptic equations, and obtained optimal error estimates for linear elliptic equations and certain nonlinear equations in standard finite element spaces. Woodward et al. [32] performed an error analysis of an expanded MFEM using the lowest-order Raviart-Thomas space for Richards equation. In [7] Arbogast et al. established the connection between the expanded MFEM and a certain cell-centered finite difference methods. A dual-dual formulation was introduced in [21] for the expanded MFEM with Raviart-Thomas spaces. The expanded formulation extends the standard mixed formulation in the sense that three variables are explicitly approximated, namely, the scalar unknown (e.g., pressure), its gradient and the velocity. The expanded MFEMs are suitable for the cases where the tensor coefficient of the underlying partial differential equations is small and even partially vanishing inside cells, which may be viewed as an extreme case of high-contrast of coefficients.

Porous media formations are often created by complex geological processes and may contain materials with a widely varying ability to transmit fluids. The permeability of the porous media may change dramatically, from almost impermeable barriers to highly permeable channels. This high-contrast of the permeability creates significant challenges for the simulation of flow through porous media. If the simulation fails to capture the influence of these barriers (e.g., shales) and channels (e.g., sand lenses),

errors in the quantities of interest will likely be unacceptably large. Moreover, if the low permeability regions are thin with a small inter-barrier spacing, a fully resolved fine-grid discretization may be difficult to obtain and costly to apply. Thus, a multiscale simulation on a coarse grid may be necessary for these situations. To simulate the flows on a coarse grid when the permeability is almost vanishing in some regions, a reduced-contrast approximation was developed in MsFEM [16] to lower the variance of the coefficients. In [2], Aarnes et al. proposed an automatic approach to detect the barrier and iteratively split the coarse cells around barriers to obtain improved solutions in mixed MsFEM. For these barrier situations, the proposed expanded mixed MsFEM can provide an easy and direct approach to perform the computation.

The purpose of this work is to develop a framework of expanded mixed MsFEMs and rigorously analyze the convergence for different multiscale cases. The work enriches the studies on mixed MsFEMs from previous works [1, 2, 14]. The multiscale phenomena can be roughly classified into two categories: separable and non-separable spatial scales. In the case of separable scales one can localize the computation of multiscale basis functions. However, these approaches usually produce resonance errors Strategies exist to reduce the resonance errors, such as the oversampling technique introduced in [23]. Recently, a new technique was proposed in [22], where a zero-th order term is artificially added to the standard multiscale basis equation [23] to make the associated Green's function decay exponentially, and consequently, the resonance error can be reduced. However, these strategies for reducing the resonance errors usually result in a nonconforming FEM, and moreover, they do not remedy the poor performance observed when the there is no scale separation. Instead, when media exhibit strong non-separable scales, some global information is needed for representing non-local effects. If the global information captures all relevant information from different scales, then resonance errors are removed and approximation accuracy is significantly improved [1, 10, 30]. If global information (or field) is used, we refer to the multiscale methods as global multiscale methods; otherwise, we refer to them as local multiscale methods. We consider the expanded mixed MsFEM for both separable and non-separable scales. Multiscale basis functions are employed for both the velocity and the gradient of the scalar. We present convergence analysis for three typical multiscale cases: periodic highly-oscillatory separable scales, $G-$convergent separable scales, and a continuum of scales. For the expanded mixed MsFEM, we consider both conforming multiscale bases and nonconforming/oversampling multiscale bases. The computation of expanded mixed MsFEM is very similar to the standard mixed MsFEM, but the expanded mixed MsFEM gives more information about the solution and provides an accurate approximation of the scalar field's gradient as well. This gradient is often needed in applications, for example, the pressure gradient is used for flows with gravity in computing upstream directions.

We consider the proposed expanded MsFEMs in the non-hybrid (standard) form and the corresponding hybrid form. The hybridization of the mixed formulation is of increasing importance to the study of mixed methods. Hybridization was initially devised by Fraejis de Veubeke [19] as an efficient implementation technique for mixed finite elements. Specifically, hybridization localizes the mass matrix on each cell, and hence, enables the local elimination of the velocity to obtain a sparse positive definite system. Later hybridization was applied to produce a better approximation of the scalar unknown over each cell. For example, Arnold and Brezzi [8] showed that using the Lagrange multiplier unknowns introduced by hybridization in a local post-processing procedure improved the accuracy of the scalar unknown. In the framework

of expanded mixed MsFEMs, we first show the equivalence between each expanded mixed MsFEM and its hybridization, and then analyze the convergence of these methods. In particular, we obtain the convergence rates of the Lagrange multipliers for each of the three multiscale cases.

The rest of the paper is organized as follows. Section 2 is devoted to formulating the expanded mixed formulation for a model elliptic equation in an abstract framework. In Section 3, we present multiscale basis functions and formulations of expanded mixed MsFEM for separable scales and continuum scales. In Section 4, we present convergence analysis for both expanded mixed MsFEMs and their hybridizations. Local multiscale methods and global multiscale methods are analyzed for the expanded mixed MsFEMs. In Section 5, the expanded mixed MsFEMs are applied to various multiscale models of flow in porous media to demonstrate their efficacy. Finally, some comments and conclusions are made.

2. Background. In this section we highlight the formulation of the expanded MFEM, and summarize important notation. We focus on the dual-dual formulation of the continuum problem because it most naturally supports our analysis. We review important results of the corresponding discretization as well.

2.1. The continuum expanded mixed formulation. Let Ω be a bounded domain in $\mathbb{R}^d$, $d = 2, 3$, with Lipschitz boundary $\partial\Omega$. For a subdomain D, $m \geq 0$ and $1 \leq p \leq \infty$, $W^{m,p}(D)$ and $L^p(D)$ denote the usual Sobolev space and Legesgue space, respectively. The norm and seminorm of $W^{m,p}$ are denoted by $\|\cdot\|_{m,p,D}$ and $|\cdot|_{m,p,D}$, respectively. When $p = 2$, $W^{m,p}(D)$ is written as $H^m(D)$ with norm $\|\cdot\|_{m,D}$ and seminorm $|\cdot|_{m,D}$. The norm of $L^2(D)$ is denoted by $\|\cdot\|_{0,D}$. We also use the following spaces

$$\begin{aligned} H_0^1(D) &:= \{q \in H^1(D) : q|_{\partial D} = 0\} \\ H(div, D) &:= \{v \in [L^2(D)]^d : \|v\|_{div,D} := \|v\|_{0,D} + \|div(v)\|_{0,D} < \infty\} \\ H^0(div, D) &:= \{v \in H(div, D) : v \cdot n|_{\partial D} = 0\}. \end{aligned}$$

For a normed space X on Ω, $\|\cdot\|_X$ denotes the underlying norm on X. We denote $X(D)$ to be the restriction of X to subdomain D. In the paper, $(\cdot, \cdot)$ is the usual $L^2(\Omega)$ inner product, and $(\cdot, \cdot)_D$ is the $L^2(D)$ inner product.

We consider the following elliptic problem

$$\begin{cases} -div(k\nabla p) = f(x) \quad \text{in} \quad \Omega \\ \qquad\qquad p = 0 \quad \text{on} \quad \partial\Omega. \end{cases} \tag{2.1}$$

We may assume k is symmetric positive definite. Let $\theta = \nabla p$ and $u = -k\theta$. The equation (2.1) can be rewritten as

$$\begin{cases} u + k\theta = 0 \\ \theta - \nabla p = 0 \\ div(u) = f. \end{cases} \tag{2.2}$$

Here u usually refers to the fluid velocity. We define the following function spaces for solutions:

$$X_1 = [L^2(\Omega)]^d, \quad X_2 = H(div, \Omega), \quad X = X_1 \times X_2, \quad Q = L^2(\Omega).$$

The expanded mixed formulation of (2.1) reads: find (θ, u, p) in $X_1 \times X_2 \times Q$, satisfying

$$\begin{cases} (k\theta, \xi) + (u, \xi) = 0 \quad \forall \xi \in X_1 \\ (\theta, \tau) + (p, div\tau) = 0 \quad \forall \tau \in X_2 \\ (divu, q) = (f, q) \quad q \in Q. \end{cases} \tag{2.3}$$

We have the following theorem, which addresses the relation between the solution of (2.1) and the solution of (2.3).

THEOREM 2.1. *(See Theorem 3.5 in [13].) If* $\big((\theta, u), p\big) \in X \times Q$ *is the solution of (2.3), then* $p \in H_0^1(\Omega)$ *is the solution of (2.1), satisfying* $\theta = \nabla p$ *and* $u = -k\theta$*. Conversely, if* $p \in H_0^1(\Omega)$ *is the solution of (2.1), then (2.3) has the solution* $\big((\theta, u), p\big) \in X \times Q$ *satisfying* $\theta = \nabla p$ *and* $u = -k\theta$*.*

For theoretical analysis, we introduce the operators associated with (2.3). Let $A_1 : X_1 \longrightarrow X_1'$ and $B_1 : X_1 \longrightarrow X_2'$, where the notation $'$ denotes the dual of a space. These are defined, respectively, by

$$\begin{aligned} [A_1(\theta), \xi] &:= (k\theta, \xi), \quad \forall \xi \in X_1\,, \\ [B_1(\theta), v] &:= (\theta, v), \quad \forall v \in X_2\,, \end{aligned}$$

from which we define $A : X \longrightarrow X'$ by

$$[A(\theta, u), (\xi, v)] := [A_1(\theta), \xi] + [B_1^*(u), \xi] + [B_1(\theta), v]\,,$$

where B_1^* is the transpose operator of B_1. Let O denote the null operator. Then A can be rewritten as

$$A = \begin{bmatrix} A_1 & B_1^* \\ B_1 & O \end{bmatrix}.$$

Let $B : X_2 \longrightarrow Q'$ and $F \in Q'$. They are defined, respectively, by

$$\begin{aligned} [B(u), q] &:= (divu, q), \quad \forall q \in Q \\ [F, q] &:= (f, q), \forall q \in Q. \end{aligned}$$

Using this operator notation, the expanded mixed formulation (2.3) is equivalent to finding $\big((\theta, u), p\big)$ in $X \times Q$ such that

$$\begin{bmatrix} A_1 & B_1^* & O \\ B_1 & O & B^* \\ O & B & O \end{bmatrix} \begin{bmatrix} \theta \\ u \\ p \end{bmatrix} = \begin{bmatrix} O \\ O \\ F \end{bmatrix}. \tag{2.4}$$

Equation (2.4) is called a dual-dual mixed formulation of (2.3) [20], since the operator A itself has a similar dual-type structure. Because the operator B satisfies a continuous inf-sup condition [12] and the operator B_1 satisfies a continuous inf-sup condition on $\ker(B)$, the system (2.4) has a unique solution $\big((\theta, u), p\big)$ in $X \times Q$. Moreover, there exists a $C > 0$, independent of the solution, such that [21]

$$\|\big((\theta, u), p\big)\|_{X \times Q} \leq C \|f\|_{0,\Omega}\,, \tag{2.5}$$

where

$$\|\big((\theta, u), p\big)\|_{X \times Q} := \|\theta\|_{X_1} + \|u\|_{X_2} + \|p\|_Q := \|\theta\|_{0,\Omega} + \|u\|_{div,\Omega} + \|p\|_{0,\Omega}\,.$$

2.2. The discrete expanded mixed formulation. Let $A_{1,h}$, $B_{1,h}$ and B_h be approximations of operators A_1, B_1 and B, respectively. Let F_h be an approximation of F. Then the numerical formulation of (2.4) reads

$$\begin{bmatrix} A_{1,h} & B_{1,h}^* & O \\ B_{1,h} & O & B_h^* \\ O & B_h & O \end{bmatrix} \begin{bmatrix} \theta_h \\ u_h \\ p_h \end{bmatrix} = \begin{bmatrix} O \\ O \\ F_h \end{bmatrix}. \tag{2.6}$$

Let $[\cdot,\cdot]_h$ be a numerical inner product. Let $X_{1,h}$, $X_{2,h}$ and Q_h be finite dimensional approximation of X_1, X_2 and Q_h, respectively. Set $X_h := X_{1,h} \times X_{2,h}$. Then we have the following abstract result for well-posedness of (2.6).

LEMMA 2.2. *[20] Assume that*

(1) there exists a positive constant C_1 independent of h such that for any $q_h \in Q_h$,

$$\sup_{v_h \in X_{2,h}\setminus\{0\}} \frac{[B_h(v_h), q_h]_h}{\|v_h\|_{X_2}} \geq C_1 \|q_h\|_Q; \tag{2.7}$$

(2) there exists a positive constant C_2 independent of h such that for any $v_h \in \ker(B_h)$

$$\sup_{\xi_h \in X_{1,h}\setminus\{0\}} \frac{[B_{1,h}(\xi_h), v_h]_h}{\|\xi_h\|_{X_1}} \geq C_2 \|v_h\|_{X_2}; \tag{2.8}$$

(3) there exist positive constant C_3 and constant C_4 independent of h such that

$$C_3\|\theta_h\|_{X_1}^2 \leq [A_{1,h}(\theta_h), \theta_h]_h \leq C_4\|\theta_h\|_{X_1}^2 \quad \textit{for} \quad \forall \theta_h \in X_{1,h}.$$

Then there exists a unique $(\theta_h, u_h, p_h) \in X_{1,h} \times X_{2,h} \times Q_h$ solution of (2.6).

We note that $\|\cdot\|_{X_2}$ should be an element broken norm, provided that $X_{2,h}$ is a nonconforming space in X_2, i.e, $X_{2,h} \not\subset X_2$. We have the following Strang-type lemma for the problem (2.6).

LEMMA 2.3. *[20] Let $\big((\theta,u),p\big) \in X \times Q$ and $\big((\theta_h,u_h),p_h\big) \in X_h \times Q_h$ be the unique solutions of (2.4) and (2.6), respectively. Then there exists $C = C(\|B_1\|, \|B\|, C_1, C_2, C_3, C_4) > 0$, where C_1, C_2, C_3 and C_4 are defined in Lemma 2.2, such that*

$$\begin{aligned} &\|\big((\theta,u),p\big) - \big((\theta_h,u_h),p_h\big)\|_{X\times Q} \leq \\ &C\Big\{ \inf_{((\xi_h,v_h),q_h)\in X_h\times Q_h} \|\big((\theta,u),p\big) - \big((\xi_h,v_h),q_h\big)\|_{X\times Q} \\ &+ \sup_{v_h \in X_{2,h}\setminus\{0\}} \frac{[-B_{1,h}(\theta) - B_h^*(p), v_h]_h}{\|v_h\|_{X_2}} \Big\}. \end{aligned} \tag{2.9}$$

Again, $\|\cdot\|_{X_2}$ in Lemma 2.3 should be an element broken norm, provided that $X_{2,h}$ is a nonconforming space in X_2. The second term on the right hand side of (2.9) is the so-called consistency error. It is easy to check that

$$\sup_{v_h \in X_{2,h}\setminus\{0\}} \frac{[-B_{1,h}(\theta) - B_h^*(p), v_h]_h}{\|v_h\|_{X_2}} = \sup_{\tilde{v}_h \in \ker(B_h)\setminus\{0\}} \frac{[-B_1(\theta), \tilde{v}_h]}{\|\tilde{v}_h\|_{X_2}}.$$

Consequently, if $\ker(B_h) \subset \ker B$, then

$$\sup_{v_h \in X_{2,h}\setminus\{0\}} \frac{[-B_{1,h}(\theta) - B_h^*(p), v_h]_h}{\|v_h\|_{X_2}} = 0,$$

which is the case for a conforming expanded mixed FEM.

As a general remark, the generic constant C is assumed to be independent of the mesh diameter h throughout the paper.

3. Formulations of expanded mixed MsFEMs. In this section, we describe how to construct multiscale basis functions for expanded mixed MsFEMs.

Let $\mathfrak{T}_h$ be a quasi-uniform partition of Ω and K be a representative coarse mesh with $diam(K) = h_K$. Let $h = \max\{h_K, K \in \mathfrak{T}_h\}$. Let (V_h, Q_h) be a classic mixed finite element space pair such as the Raviart-Thomas, Brezzi-Douglas-Marini or Brezzi-Douglas-Fortin-Marini spaces (cf. [12]). In this section, we present multiscale basis functions for standard local expanded mixed MsFEM, oversampling expanded mixed MsFEM, and global expanded mixed MsFEM.

3.1. Local expanded mixed MsFEM. Let $V_h(K) := V_h|_K$ (the finite element velocity space localized on K) and $\chi^K \in V_h(K)$ be a velocity basis function defined on K. Following the mixed MsFEMs developed in [14], we define the multiscale basis equation for the local expanded mixed MsFEM in the following way:

$$\begin{cases} \psi_\chi^K + k\eta_\chi^K = 0 \quad \text{in} \quad K \\ \eta_\chi^K - \nabla\phi_\chi^K = 0 \quad \text{in} \quad K \\ div(\psi_\chi^K) = div\chi^K \quad \text{in} \quad K \\ \psi_\chi^K \cdot n_{\partial K} = \chi^K \cdot n_{\partial K} \quad \text{on} \quad \partial K, \end{cases} \tag{3.1}$$

where $n_{\partial K}$ is the outward unit normal to ∂K. We can obtain different mixed MsFEM basis functions corresponding to different choices of χ^K. Chen and Hou [14] choose χ^K to be the lowest Raviart-Thomas basis. The weak expanded mixed formulation of (3.1) is to find $\big((\eta_\chi^K, \psi_\chi^K), \phi_\chi^K\big) \in X(K) \times Q(K)/R$ such that

$$\begin{cases} (k\eta_\chi^K, \xi) + (\psi_\chi^K, \xi) = 0, \quad \forall \xi \in [L^2(K)]^d \\ (\eta_\chi^K, \tau) + (\phi_\chi^K, div\tau) = 0, \quad \forall \tau \in H^0(div, K) \\ (div\psi_\chi^K, q) = (div\chi^K, q), \quad \forall q \in L^2(K) \end{cases} \tag{3.2}$$

with $\psi_\chi^K \cdot n_{\partial K} = \chi^K \cdot n_{\partial K}$ on ∂K. The function η_χ^K is a basis function for the gradient variable θ and ψ_χ^K is a basis function for velocity u. We define finite element spaces for the local expanded mixed MsFEM as follows:

$$\begin{aligned} X_{1,h}^l &:= \{\theta \in [L^2(\Omega)]^d : \theta|_K \in span\{\eta_\chi^K\} \quad \text{for each } K \in \mathfrak{T}_h\} \\ X_{2,h}^l &:= \{u \in H(div, \Omega) : u|_K \in span\{\psi_\chi^K\} \quad \text{for each } K \in \mathfrak{T}_h\} \\ X_h^l &:= X_{1,h}^l \times X_{2,h}^l. \end{aligned}$$

The finite element space for pressure in the expanded mixed MsFEM is Q_h, which is the same as in the classic mixed finite element pairs. On each coarse element K, the velocity basis functions are associated with its faces. Therefore, velocity basis functions of $X_{2,h}^l$ have the support of two coarse elements sharing a common interface. However, the basis functions of $X_{1,h}^l$ are supported in only one coarse element. Each basis function of $X_{1,h}^l$ is associated with a velocity basis function via $\psi_\chi^K = -k\eta_\chi^K$, but it is restricted to only one coarse element K.

The local expanded mixed MsFEM formulation of the global problem (2.3) reads: find $\big((\theta_h^l, u_h^l), p_h^l\big) \in X_h^l \times Q_h$ such that

$$\begin{cases} (k\theta_h^l, \xi_h) + (u_h^l, \xi_h) = 0 \quad \forall \xi_h \in X_{1,h}^l \\ (\theta_h^l, \tau_h) + (p_h^l, div\tau_h) = 0 \quad \forall \tau_h \in X_{2,h}^l \\ (divu_h^l, q_h) = (f, q_h) \quad q \in Q_h \end{cases} \tag{3.3}$$

subject to the global boundary conditions.

It is well known [13] that the linear system of equations in the expanded mixed FEM produces an indefinite matrix, which is a considerable source of trouble when solving the linear system. We can introduce Lagrange multipliers on interfaces of cells and localize mass matrix to each element to obtain a sparse symmetric positive definite system by elimination, which is suitable for many linear solvers. This will give rise to a hybrid formulation. To this end we require some further notations.

For the hybrid formulation we define the MsFEM velocity space to be $\tilde{X}^l_{2,h}$, whose normal components are not necessarily continuous on $\mathcal{F}_h$, the collection interior interfaces of $\mathfrak{T}_h$. They are defined as follows:

$$\tilde{X}^l_{2,h} := \{u \in [L^2(\Omega)]^d : u|_K \in span\{\psi^K_\chi\} \quad \text{for each } K \in \mathfrak{T}_h\}$$

We note that basis functions in $\tilde{X}^l_{2,h}$ do not require normal continuity. The basis function in $\tilde{X}^l_{2,h}$ is supported on a coarse grid, and this is different from the basis function in $X^l_{2,h}$ whose support is two coarse cells sharing the common face. We note that

$$X^l_{2,h} = \tilde{X}^l_{2,h} \cap H(div, \Omega).$$

The finite element space for the Lagrange multiplier is defined as

$$\Pi^l_h := \big\{\pi \in L^2(\mathcal{F}_h) : \pi|_e \in X^l_{2,h} \cdot n_e \quad \text{for each } e \in \mathcal{F}_h, \quad \pi|_e = 0 \quad \text{for } e \subset \partial\Omega\big\}.$$

Define the operator $C^l_h : \tilde{X}^l_{2,h} \longrightarrow (\Pi^l_h)'$ by

$$[C^l_h(\tau_h), \pi_h] = \sum_K (\tau_h \cdot n_{\partial K}, \pi_h)_{\partial K}, \quad \forall \tau_h \in \tilde{X}^l_{2,h}, \pi_h \in \Pi^l_h. \tag{3.4}$$

The hybridization of local expanded mixed MsFEM formulation of (3.3) reads: find $(\bar{\theta}^l_h, \bar{u}^l_h, \bar{p}^l_h, \lambda^l_h) \in X^l_h \times \tilde{X}^l_{2,h} \times Q_h \times \Pi^l_h$ such that

$$\begin{cases} (k\bar{\theta}^l_h, \xi_h) + (\bar{u}^l_h, \xi_h) = 0 \quad \forall \xi_h \in X^l_{1,h} \\ (\bar{\theta}^l_h, \tau_h) + \sum_K (\bar{p}^l_h, div\tau_h) = [C^l_h(\tau_h), \lambda^l_h] \quad \forall \tau_h \in \tilde{X}^l_{2,h} \\ \sum_K (div\bar{u}^l_h, q_h) = (f, q_h) \quad q \in Q_h \\ [C^l_h(\bar{u}^l_h), \pi_h] = 0 \quad \pi_h \in \Pi^l_h. \end{cases} \tag{3.5}$$

3.2. Oversampling expanded mixed MsFEM. If the equation (3.1) is solved in a block S larger than K, and the interior information of the solution is taken to construct the basis functions in K, then this results in the oversampling technique introduced in [23, 14]. We note that oversampling MsFEM is a modified local MsFEM. Using the oversampling can reduce resonance error.

Here we follow the outline in [14] to present the oversampling multiscale basis functions. Let $\big((\eta^S_\chi, \psi^S_\chi), \phi^S_\chi\big) \in X(S) \times Q(S)/R$ be the solution of the equation

$$\begin{cases} \psi^S_\chi + k\eta^S_\chi = 0 \quad \text{in} \quad S \\ \eta^S_\chi - \nabla\phi^S_\chi = 0 \quad \text{in} \quad S \\ div(\psi^S_\chi) = div\chi^S \quad \text{in} \quad S \\ \psi^S_\chi \cdot n_{\partial K} = \chi^S \cdot n_{\partial K} \quad \text{on} \quad \partial S. \end{cases} \tag{3.6}$$

Let j and l be indices of faces of K. We define

$$\bar{\psi}^K_{\chi_j} := \sum_l c_{jl}\psi^S_{\chi_l}|_K, \quad \bar{\eta}^K_{\chi_j} := \sum_l c_{jl}\eta^S_{\chi_l}|_K, \tag{3.7}$$

where the constants c_{jl} are chosen such that

$$\chi^K_j = \sum_l c_{jl}\chi^S_l|_K. \tag{3.8}$$

We define

$$\tilde{X}^{os}_{2,h} := \{u \in [L^2(\Omega)]^d : u|_K \in span\{\bar{\psi}^K_\chi\} \quad \text{for each } K \in \mathfrak{T}_h\}.$$

We introduce an operator $\mathcal{M}_h : \tilde{X}^{os}_{2,h} \longrightarrow V_h$ whose local form is defined by

$$\mathcal{M}_h|_K\big(\sum_j c_j\bar{\psi}^K_{\chi_j}\big) = \sum_j c_j\chi^K_j. \tag{3.9}$$

Then we define finite element spaces for the oversampling expanded mixed MsFEM as follows:

$$X^{os}_{1,h} := \{\theta \in [L^2(\Omega)]^d : \theta|_K \in span\{\bar{\eta}^K_\chi\} \quad \text{for each } K \in \mathfrak{T}_h\}$$
$$X^{os}_{2,h} := \{u_h \in \tilde{X}^{os}_{2,h} : \mathcal{M}_h u_h \in V_h \subset H(div,\Omega)\}.$$

Here, $\mathcal{M}_h u_h \in V_h$ is to impose some intrinsic continuity of the normal components of velocity multiscale basis functions across the interfaces $\mathcal{F}_h$. However, $X^{os}_{2,h} \not\subset H(div,\Omega)$ and so the oversampling multiscale method is nonconforming. The expanded oversampling mixed MsFEM formulation of the global problem (2.3) reads: find $(\theta^{os}_h, u^{os}_h, p^{os}_h) \in X^{os}_{1,h} \times X^{os}_{2,h} \times Q_h$ such that

$$\begin{cases} (k\theta^{os}_h, \xi_h) + (u^{os}_h, \xi_h) = 0 \quad \forall \xi_h \in X^{os}_{1,h} \\ (\theta^{os}_h, \tau_h) + \sum_K (p^{os}_h, div\tau_h)_K = 0 \quad \forall \tau_h \in X^{os}_{2,h} \\ \sum_K (divu^{os}_h, q_h)_K = (f, q_h) \quad q_h \in Q_h \end{cases} \tag{3.10}$$

subject to the global boundary conditions.

We define operator $C^{os}_h : \tilde{X}^{os}_{2,h} \longrightarrow (\Pi^l_h)'$ by

$$[C^{os}_h(\tau_h), \pi_h] := \sum_K (\mathcal{M}_h(\tau_h)\cdot n, \pi_h)_{\partial K}, \quad \forall \tau_h \in \tilde{X}^{os}_{2,h}, \pi_h \in \Pi^l_h.$$

Then the hybridization of (3.10) is to find $(\theta^{os}_h, u^{os}_h, p^{os}_h, \lambda^{os}_h) \in X^{os}_{1,h} \times \tilde{X}^{os}_{2,h} \times Q_h \times \Pi^l_h$ such that

$$\begin{cases} (k\theta^{os}_h, \xi_h) + (u^{os}_h, \xi_h) = 0 \quad \forall \xi_h \in X^{os}_{1,h} \\ (\theta^{os}_h, \tau_h) + \sum_K (p^{os}_h, div\tau_h)_K = [C^{os}_h(\tau_h), \lambda^{os}_h] \quad \forall \tau_h \in \tilde{X}^{os}_{2,h} \\ \sum_K (divu^{os}_h, q_h)_K = (f, q_h) \quad q_h \in Q_h \\ [C^{os}_h(u_h), \pi_h] = 0 \quad \pi_h \in \Pi^l_h. \end{cases} \tag{3.11}$$

3.3. Global expanded mixed MsFEM. To remove the resonance error and substantially improve the accuracy, we can use global information to construct the multiscale basis functions. Suppose that there exist global fields $u_1, \cdots, u_N$ that capture the non-local features of the solution of equation (2.1). Following the global mixed MsFEM framework proposed in [1], we define the multiscale basis equations for the global expanded mixed MsFEM by

$$\begin{cases} \psi_{i,\chi}^K + k\eta_{i,\chi}^K = 0 \quad \text{in} \quad K \\ \eta_{i,\chi}^K - \nabla\phi_{i,\chi}^K = 0 \quad \text{in} \quad K \\ div(\psi_{i,\chi}^K) = div\chi^K \quad \text{in} \quad K \\ \psi_{i,\chi}^K \cdot n_{\partial K} = b_i^{\partial K} \quad \text{on} \quad \partial K, \end{cases} \tag{3.12}$$

where $b_i^{\partial K} := \dfrac{\int_{\partial K} \chi^K \cdot n_{\partial K} ds}{\int_{\partial K} u_i \cdot n_{\partial K} ds} u_i \cdot n_{\partial K}$ and $i = 1, ..., N$ are indices of the global information. References [1, 10, 30] provide some options for the global fields. To reduce the computational cost of using global fields, we can pre-compute these fields $u_1, \cdots, u_N$ at some intermediate scale [26].

The finite element spaces for the global expanded mixed MsFEM are defined by

$$\begin{aligned} X_{1,h}^g &:= \{\theta \in [L^2(\Omega)]^d : \theta|_K \in span\{\eta_{i,\chi}^K\} \quad \text{for each } K \in \mathfrak{T}_h\} \\ X_{2,h}^g &:= \{u \in H(div, \Omega) : u|_K \in span\{\psi_{i,\chi}^K\} \quad \text{for each } K \in \mathfrak{T}_h\} \\ X_h^g &:= X_{1,h}^g \times X_{2,h}^g. \end{aligned}$$

Consequently the global expanded mixed MsFEM formulation of the global problem (2.3) reads: find $\left((\theta_h^g, u_h^g), p_h^g\right) \in X_h^g \times Q_h$ such that

$$\begin{cases} (k\theta_h^g, \xi_h) + (u_h^g, \xi_h) = 0 \quad \forall \xi_h \in X_{1,h}^g \\ (\theta_h^g, \tau_h) + (p_h^g, div\tau_h) = 0 \quad \forall \tau_h \in X_{2,h}^g \\ (divu_h^g, q_h) = (f, q_h) \quad q \in Q_h \end{cases} \tag{3.13}$$

subject to the global boundary conditions.

We define the MsFEM velocity space $\tilde{X}_{2,h}^g$ and the finite element space Π_h^g of the Lagrange multipliers for the hybrid formulation of (3.13) by

$$\begin{aligned} \tilde{X}_{2,h}^g &:= \{u \in [L^2(\Omega)]^d : u|_K \in span\{\psi_{i,\chi}^K\} \quad \text{for each } K \in \mathfrak{T}_h\} \\ \Pi_h^g &:= \left\{\pi \in L^2(\mathcal{F}_h) : \pi|_e \in X_{2,h}^g \cdot n_e \quad \text{for each } e \in \mathcal{F}_h, \quad \pi|_e = 0 \quad \text{for } e \subset \partial\Omega\right\}. \end{aligned}$$

The functions in $\tilde{X}_{2,h}^g$ may not have normal continuity. The relation between $X_{2,h}^g$ and $\tilde{X}_{2,h}^g$ is expressed by the identity $X_{2,h}^g = \tilde{X}_{2,h}^g \cap H(div, \Omega)$.

Let the operator $C_h^g : \tilde{X}_{2,h}^g \longrightarrow (\Pi_h^g)'$ be defined in a similar way to (3.4). Then the hybridization of the global expanded mixed MsFEM formulation of (3.13) reads: find $(\bar{\theta}_h^g, \bar{u}_h^g, \bar{p}_h^g, \lambda_h^g) \in X_h^g \times \tilde{X}_{2,h}^g \times Q_h \times \Pi_h^g$ such that

$$\begin{cases} (k\bar{\theta}_h^g, \xi_h) + (\bar{u}_h^g, \xi_h) = 0 \quad \forall \xi_h \in X_{1,h}^g \\ (\bar{\theta}_h^g, \tau_h) + \sum_K (\bar{p}_h^g, div\tau_h) = [C_h^g(\tau_h), \lambda_h^g] \quad \forall \tau_h \in \tilde{X}_{2,h}^g \\ \sum_K (div\bar{u}_h^g, q_h) = (f, q_h) \quad q \in Q_h \\ [C_h^l(\bar{u}_h^g), \pi_h] = 0 \quad \pi_h \in \Pi_h^g. \end{cases} \tag{3.14}$$

We note that (3.5), (3.11) and (3.14) can be rewritten as the operator formulation

$$\begin{bmatrix} A_{1,h} & B_{1,h}^* & O & O \\ B_{1,h} & O & B_h^* & -C_h^* \\ O & B_h & O & O \\ O & -C_h & O & O \end{bmatrix} \begin{bmatrix} \bar{\theta}_h \\ \bar{u}_h \\ \bar{p}_h \\ \lambda_h \end{bmatrix} = \begin{bmatrix} O \\ O \\ F_h \\ O \end{bmatrix}. \tag{3.15}$$

This is actually the hybrid approximation of the operator equation (2.6).

4. Convergence analysis. We will focus on the analysis of the local expanded mixed MsFEM. The analysis of the oversampling expanded mixed MsFEM and the global expanded mixed MsFEM is very similar to the local expanded mixed MsFEM but requires additional notation and definitions. We sketch the analysis of the oversampling expanded mixed MsFEM and global expanded mixed MsFEM and present their convergence results. For the local expanded mixed MsFEM, we consider microscales that can be treated in terms of periodic homogenization and $G-$convergent homogenization.

For the analysis, we will focus on the case when the velocity space on K, $V_h(K)$, is the lowest-order Raviart-Thomas space (RT_0) and $\chi^K \in V_h(K)$. We use χ^K to build the source term and boundary conditions for the MsFEM basis defined in equation (3.1).

4.1. Inf-sup condition for expanded mixed MsFEMs. In this subsection, we discuss the inf-sup condition associated with problem (3.3). To simplify the presentation, we define three discrete operators associated with (3.3). Specifically, let $A_{1,h} : X_{1,h}^l \longrightarrow X_{1,h}'$, $B_{1,h} : X_{1,h}^l \longrightarrow X_{2,h}'$ and $B_h : X_{2,h}^l \longrightarrow Q_h'$, then the operators are defined as

$$\begin{aligned} [A_{1,h}(\theta), \xi] &:= (k\theta, \xi), \quad \forall \xi \in X_{1,h}^l \\ [B_{1,h}(\theta), v] &:= (\theta, v), \quad \forall v \in X_{2,h}^l \\ [B_h(u), q] &:= (div(u), q), \quad \forall q \in Q_h. \end{aligned}$$

By Lemma 2.2, we require that the operator $A_{1,h}$ is bounded and positive for well-posedness of problem (3.3). If k satisfies the assumption

$$k_{\min}|\zeta|^2 \leq \zeta^T k(x)\zeta \leq k_{\max}|\zeta|^2 \quad \text{for } \forall \zeta \in \mathbb{R}^d \text{ and } \forall x \in \Omega, \tag{4.1}$$

then the operator $A_{1,h}$ is bounded and positive. However, we can weaken the assumption (4.1); for example, $k(x)$ may be partially vanishing inside fine cells and positive and bounded everywhere else. Then the operator $A_{1,h}$ is still positive and bounded. For simplicity of presentation, we use assumption (4.1) for the analysis.

We have the following lemma for the discrete inf-sup condition of problem (3.3).

LEMMA 4.1. *For any $q_h \in Q_h$, there exists a positive constant C_1 independent of h such that*

$$\sup_{v_h \in X_{2,h}^l \setminus \{0\}} \frac{[B_h(v_h), q_h]}{\|v_h\|_{X_2}} \geq C_1 \|q_h\|_Q. \tag{4.2}$$

Let $\ker(B_h)$ *be the kernel of the operator B_h. Then for any $v_h \in \ker(B_h)$, there exists a positive constant C_2 independent of h such that*

$$\sup_{\xi_h \in X_{1,h}^l \setminus \{0\}} \frac{[B_{1,h}(\xi_h), v_h]}{\|\xi_h\|_{X_1}} \geq C_2 \|v_h\|_{X_2}. \tag{4.3}$$

Proof. We define $v_h^* \in V_h$, whose localization on K is $v_h^*|_K = \sum_j a_j^K \chi_j^K \in V_h(K)$, where j is the index of a face of K. Consider a map M whose local form is defined by $M_K v_h^* = \sum_j a_j^K \psi_{\chi_j}^K \in X_{2,h}^l(K)$. Then $M : V_h \longrightarrow X_{2,h}^l$ is a one-to-one map. It is easy to check for any $v_h^* \in V_h$,

$$div(Mv_h^*) = div(v_h^*) \ \text{ in } \ K. \tag{4.4}$$

Let $z^K = \sum_j a_j^K \phi_{\chi_j}^K$. Then $M_K v_h^* = -k\nabla z^K$ and we have

$$\begin{aligned}
&\|M_K v_h^*\|_{0,K}^2 = \int_K k\nabla z^K \cdot k\nabla z^K dx \le C\int_K k\nabla z^K \cdot \nabla z^K dx \\
&= -C\int_K M_K v_h^* \cdot \nabla z^K dx = C(\int_K div(M_K v_h^*) z^K dx - \int_{\partial K} (M_K v_h^*)\cdot n z^K ds) \\
&= C(\int_K div(v_h^*) z^K dx - \int_{\partial K} v_h^* \cdot n z^K ds) = -C\int_K v_h^* \cdot \nabla z^K dx \\
&= C\int_K v_h^* \cdot k^{-1} M_K v_h^* dx \le C\|v_h^*\|_{0,K}\|M_K v_h^*\|_{0,K}.
\end{aligned} \tag{4.5}$$

This gives $\|M_K v_h^*\|_{0,K} \le C\|v_h^*\|_{0,K}$. Consequently, combining with (4.4) implies that for any $v_h^* \in V_h^*$,

$$\|Mv_h^*\|_{X_2} \le C\|v_h^*\|_{X_2}. \tag{4.6}$$

Consequently, since the inf-sup condition holds for the classic mixed FE pair (V_h, Q_h), it follows that for any $q_h \in Q_h$

$$\begin{aligned}
\sup_{v_h \in X_{2,h}^l \setminus \{0\}} \frac{(divv_h, q_h)}{\|v_h\|_{X_2}} &\ge \sup_{v_h^* \in V_h \setminus \{0\}} \frac{(div(Mv_h^*), q_h)}{\|Mv_h^*\|_{X_2}} \\
&\ge \frac{1}{C} \sup_{v_h^* \in V_h \setminus \{0\}} \frac{(divv_h^*, q_h)}{\|v_h^*\|_{X_2}} \ge \frac{C^*}{C}\|q_h\|_Q,
\end{aligned} \tag{4.7}$$

where we have used (4.6) in the second step. The proof of (4.2) is complete.

It is obvious that by definition

$$\ker(B_h) = \{v_h \in X_{2,h}^l : div(v_h) = 0\},$$

and hence $\ker(B_h) \subset X_{2,h}^l \subset X_{1,h}^l$. Then for any $v_h \in \ker(B_h)$,

$$\sup_{\xi_h \in X_{1,h}^l \setminus \{0\}} \frac{[B_{1,h}(\xi_h), v_h]}{\|\xi_h\|_{X_1}} = \sup_{\xi_h \in X_{1,h}^l \setminus \{0\}} \frac{(\xi_h, v_h)}{\|\xi_h\|_{X_1}} = \|v_h\|_{0,\Omega} = \|v_h\|_{X_2},$$

which completes the proof of (4.3). □

Using Lemma 2.2, Lemma 4.1 and Lemma 2.3 gives the following theorem.

THEOREM 4.2. *The problem (3.3) has a unique solution* $\big((\theta_h^l, u_h^l), p_h^l\big) \in X_h^l \times Q_h$. *Let* $\big((\theta, u), p\big)$ *be the solution of (2.3). Then there exists a positive constant* C *independent of* h *such that*

$$\|\big((\theta, u), p\big) - \big((\theta_h^l, u_h^l), p_h^l\big)\|_{X\times Q} \le C \inf_{\big((\xi_h, v_h), q_h\big) \in X_h^l \times Q_h} \|\big((\theta, u), p\big) - \big((\xi_h, v_h), q_h\big)\|_{X\times Q}. \tag{4.8}$$

Following the proof of Lemma 4.1 and using the argument of Lemma 4.4 in [14], we can obtain the inf-sup condition for the oversampling expanded mixed MsFEM problem (3.10). Then applying Lemma 2.3 to (3.10), we have the estimate

$$\begin{aligned}
&\sum_K \|\big((\theta,u),p\big)-\big((\theta_h^{os},u_h^{os}),p_h^{os}\big)\|_{X(K)\times Q(K)}\\
&\leq C\big\{\inf_{(\xi_h,v_h,q_h)\in X_{1,h}^{os}\times X_{2,h}^{os}\times Q_h}\sum_K\|((\theta,u),p)-((\xi_h,v_h),q_h)\|_{X(K)\times Q(K)}\big\}\\
&+\sum_{v_h\in X_{2,h}^{os}\setminus\{0\}}\frac{-(\theta,v_h)-\sum_K(div(v_h),p)}{\sum_K\|v_h\|_{div,K}}.
\end{aligned}\tag{4.9}$$

The last term of (4.9) is the consistency error caused by the oversampling velocity space.

Under suitable conditions described in [1], we can similarly obtain the inf-sup conditions for the global expanded mixed multiscale finite element problem (3.13) and the Céa-type estimate,

$$\|\big((\theta,u),p\big)-\big((\theta_h^g,u_h^g),p_h^g\big)\|_{X\times Q}\leq C\inf_{\big((\xi_h,v_h),q_h)\big)\in X_h^g\times Q_h}\|\big((\theta,u),p\big)-\big((\xi_h,v_h),q_h)\big)\|_{X\times Q}.\tag{4.10}$$

4.2. Equivalence between expanded mixed MsFEM and its hybridization. In this subsection, we show that expanded mixed MsFEM formulation and its hybridization produce the same vector functions (i.e., the gradient of pressure and velocity). The result will be helpful to proceed with the convergence analysis for expanded mixed MsFEM and its hybrid formulation. For simplicity, we focus on the case of local mixed MsFEM.

We first have the following lemma for operator C_h^l.

LEMMA 4.3. *Let C_h^l be defined in (3.4). Then*

$$\ker C_h^l = X_{2,h}^l,\quad \ker(C_h^l)^* = \{0\}.$$

Proof. By definition of $X_{2,h}^l$ and (3.4), it immediately follows that

$$\ker C_h^l = X_{2,h}^l.$$

Let K^* be any cell in $\mathfrak{T}_h$ and e^* be any face of K^*. Let $\tau^*\in\tilde{X}_{2,h}^l$ be such that

$$\tau_h^*|_K = 0\quad \forall K\neq K^*$$

and defined on K^* by

$$\begin{cases}\tau_h^*\cdot n_e &= 0\quad \text{for}\quad e\neq e^*\\ \tau_h^*\cdot n_{e^*} &= \chi_{e^*}^{K^*}\cdot n_{e^*},\end{cases}$$

where $\chi_{e^*}^{K^*}\in V_h(K^*)$ is any basis function associated with face e^*. Then $[(C_h^l)^*(\pi_h),\tau_h^*]=0$ means that $(\chi_{e^*}^{K^*}\cdot n,\pi_h)_{e^*}=0$ for any basis function $\chi_{e^*}^{K^*}\in V_h(K^*)$ associated with face e^*. The classic mixed FEM theory implies that $\pi_h=0$ on e^*. Since K^* is any cell in $\mathfrak{T}_h$ and e^* is an arbitrary interface, $\pi_h=0$ on $\mathcal{F}_h$. This completes the proof.

□

Next we show that problem (3.3) and problem (3.5) produce the same solution.

THEOREM 4.4. *Problem* (3.3) *has a unique solution* $\big((\theta_h^l, u_h^l), p_h^l\big) \in X_h^l \times Q_h$. *Problem (3.5) has a unique solution* $(\bar{\theta}_h^l, \bar{u}_h^l, \bar{p}_h^l, \lambda_h^l) \in X_{1,h}^l \times \tilde{X}_{2,h}^l \times Q_h \times \Pi_h^l$. *Moreover,* $\big((\bar{\theta}_h^l, \bar{u}_h^l), \bar{p}_h^l\big) = \big((\theta_h^l, u_h^l), p_h^l\big)$.

Proof.

Following the proof of Theorem 3.1 in [7] and using a standard duality argument, we obtain that

$$\|\theta_h^l\|_{0,\Omega} + \|u_h^l\|_{0,\Omega} + \|p_h^l\|_{0,\Omega} \leq C\|f\|_{0,\Omega},$$

which shows (3.3) has a unique solution by setting $f = 0$.

Let $\big((\theta_h^l, u_h^l), p_h^l\big)$ be the unique solution of (3.3). We define a linear operator by

$$L(\tau_h) = (\theta_h^l, \tau_h) + \sum_K (p_h^l, div\tau_h)_K, \quad \forall \tau_h \in \tilde{X}_{2,h}^l. \tag{4.11}$$

It is clear that $L(\tau_h) = 0$ for all $\tau_h \in X_{2,h}^l$, i.e, $X_{2,h}^l \subset \ker L$ and

$$L \in [\ker(C_h^l)]^\perp := \{l \in (\tilde{X}_{2,h}^l)' :< l, \tau_h >= 0, \quad \forall \tau_h \in \ker(C_h^l)\}.$$

By the Closed Range Theorem, it follows that

$$[\ker(C_h^l)]^\perp = \Re((C_h^l)^*).$$

This means that there exists a $\lambda_h \in \Pi_h^l$ such that $(C_h^l)^*(\lambda_h) = L$, which gives

$$L(\tau_h) = [C_h^l(\tau_h), \lambda_h^l] \quad \forall \tau_h \in \tilde{X}_{2,h}^l. \tag{4.12}$$

Then by Lemma 4.3, λ_h^l is unique. Combining (4.11) and (4.12) gives

$$(\theta_h^l, \tau_h) + \sum_K (p_h^l, div\tau_h)_K = [C_h^l(\tau_h), \lambda_h^l] \quad \forall \tau_h \in \tilde{X}_{2,h}^l. \tag{4.13}$$

The equation (4.13) is exactly the same as the second equation in (3.5). The fourth equation in (3.5) and Lemma 4.3 show that $\bar{u}_h \in X_{2,h}^l$. By uniqueness of solutions of (3.3) and uniqueness of λ_h^l, we immediately obtain that $\big((\bar{\theta}_h^l, \bar{u}_h^l), \bar{p}_h^l\big)$ is unique and

$$\big((\bar{\theta}_h^l, \bar{u}_h^l), \bar{p}_h^l\big) = \big((\theta_h^l, u_h^l), p_h^l\big).$$

□

By a procedure similar to Theorem 4.4, we have the following theorems for oversampling expanded mixed MsFEM and global expanded mixed MsFEM, respectively.

THEOREM 4.5. *Problem (3.11) has a unique solution* $(\bar{\theta}_h^{os}, \bar{u}_h^{os}, \bar{p}_h^{os}, \lambda_h^{os}) \in X_{1,h}^{os} \times \tilde{X}_{2,h}^{os} \times Q_h \times \Pi_h^l$. *Moreover,* $\big((\bar{\theta}_h^{os}, \bar{u}_h^{os}), \bar{p}_h^{os}\big) = \big((\theta_h^{os}, u_h^{os}), p_h^{os}\big)$, *where* $\big((\theta_h^{os}, u_h^{os}), p_h^{os}\big)$ *is the unique solution of problem (3.10).*

THEOREM 4.6. *Problem (3.14) has a unique solution* $(\bar{\theta}_h^g, \bar{u}_h^g, \bar{p}_h^g, \lambda_h^g) \in X_{1,h}^g \times \tilde{X}_{2,h}^g \times Q_h \times \Pi_h^g$. *Moreover,* $\big((\bar{\theta}_h^g, \bar{u}_h^g), \bar{p}_h^g\big) = \big((\theta_h^g, u_h^g), p_h^g\big)$, *where* $\big((\theta_h^g, u_h^g), p_h^g\big)$ *is the unique solution of* (3.13).

Theorem 4.4, Theorem 4.5 and Theorem 4.6 allow us to identify $\big((\bar{\theta}_h^l, \bar{u}_h^l), \bar{p}_h^l\big)$ with $\big((\theta_h^l, u_h^l), p_h^l\big)$, $\big((\bar{\theta}_h^{os}, \bar{u}_h^{os}), \bar{p}_h^{os}\big)$ with $\big((\theta_h^{os}, u_h^{os}), p_h^{os}\big)$, and $\big((\bar{\theta}_h^g, \bar{u}_h^g), \bar{p}_h^g\big)$ with $\big((\theta_h^g, u_h^g), p_h^g\big)$,

respectively. So we can drop the upper bars in corresponding hybrid systems (3.5), (3.11), and (3.14), respectively. We note that $\bar{u}_h^l = u_h^l$ is an identity in the sense of vector-valued functions. However, the corresponding coefficient arrays on their numerical representations are not equal to each other, because $dim(X_{2,h}^l) \neq dim(\tilde{X}_{2,h}^l)$. The same relationships hold for the oversampling expanded mixed MsFEM and the global expanded mixed MsFEM as well. Thus, to simplify the notation, we will drop the upper bars from (3.5), (3.11) and (3.14) in the rest of the paper.

4.3. Error analysis for the periodic case. In this subsection, we consider the case $k(x) = k(\frac{x}{\epsilon})$, where the parameter ϵ characterizes small scales representing small physical lengths. To highlight the dependence on the small parameter ϵ, we rewrite the solution of (2.3) as $\big((\theta_\epsilon, u_\epsilon), p_\epsilon\big)$. We present an error analysis when the ϵ scales are periodic. The local expanded mixed MsFEM and the oversampling expanded mixed MsFEM will be considered in the following subsections.

We briefly recall the relevant homogenization results for the periodic case. Specifically, let $y = \frac{x}{\epsilon}$ and $k(y)$ be a periodic function in the unit cube $Y = [0,1]^d$. In this case, we can compute k^* in the following way. Let $\mathcal{N} = \{\mathcal{N}_1, \cdots, \mathcal{N}_d\}$ solve the auxiliary equations

$$\begin{cases} -div_y(k(y)\nabla\mathcal{N}_i) &= div_y(k(y)e_i) \ \text{ in } \ Y \\ \langle \mathcal{N}_i(y)\rangle_Y &= 0. \end{cases} \tag{4.14}$$

Here e_i $(i = 1, \cdots, d)$ is the unit vector in $\mathbb{R}^d$. Then the homogenized tensor k^* is defined as (see, e.g., [27])

$$k^* = \langle k(\nabla\mathcal{N} + I)\rangle_Y.$$

Let p^* solve the homogenized equation of (2.1) by

$$\begin{cases} -div(k^*\nabla p^*) = f(x) \quad \text{in} \quad \Omega \\ p^* = 0 \quad \text{on} \quad \partial\Omega. \end{cases} \tag{4.15}$$

We define the homogenized velocity u^* by $u^* := -k^*\nabla p^*$.

Since we consider $\chi^K \in V_h(K) := RT_0(K)$, we have $div\chi^K = \frac{1}{|K|}$ and $\chi_e^K \cdot n_e = \frac{1}{|e|}$ on e and 0 otherwise. For this case, Q_h is a piecewise constant space.

4.3.1. Analysis of local expanded MsFEM. Let $\mathcal{I}_h^* : [H^1(\Omega)]^d \longrightarrow V_h$ be the interpolation operator of RT_0 for velocity. Let $\mathcal{P}_h : L^2(\Omega) \longrightarrow Q_h$ be an orthogonal L^2 projection. We define the multiscale interpolation operator $\mathcal{I}_h : [H^1(\Omega)]^d \longrightarrow \tilde{X}_{2,h}^l$ for velocity by

$$\mathcal{I}_h(v) := \sum_{e\in\mathcal{F}_h} (\int_e v \cdot n_e ds)\psi_{\chi_e},$$

where ψ_{χ_e} is a multiscale velocity basis function associated with interface e. We define the L^2 interface projection $\mathcal{P}_\partial : L^2(\mathcal{F}_h) \longrightarrow \Pi_h^l$ such that

$$(\mathcal{P}_\partial p - p, \pi_h)_e = 0 \quad \forall \pi_h \in \Pi_h^l \quad \text{ and } \quad \forall e \in \mathcal{F}_h.$$

This interface projection implies that $\mathcal{P}_\partial p|_e = (\int_e p ds)\chi_e \cdot n_e$. We define a discrete norm on $L^2(\mathcal{F}_h)$ by

$$\|\pi\|_{-\frac{1}{2},h}^2 = \sum_{K\in\mathfrak{T}} \sum_{e\subset\partial K} h_K \|\pi\|_{0,e}^2.$$

LEMMA 4.7. *If χ_e^K is a lowest Raviart-Thomas element, then the corresponding multiscale basis function $\psi_{\chi_e}^K$ satisfies*

$$\|\psi_{\chi_e}^K\|_{0,K} \leq C|e|^{-\frac{1}{2}} h_K^{\frac{1}{2}}. \tag{4.16}$$

Proof. By basis equation (3.1), it follows that

$$\begin{cases} -div(k\nabla\phi_{\chi_e}^K) = \dfrac{1}{|K|} & \text{in K} \\ -k\nabla\phi_{\chi_e}^K \cdot n_e = \dfrac{1}{|e|} & \text{on } e \\ -k\nabla\phi_{\chi_e}^K \cdot n = 0 & \text{on } \partial K \setminus e \\ \dfrac{1}{|K|}\displaystyle\int_K \phi_{\chi_e}^K = 0. \end{cases}$$

Multiplying $\phi_{\chi_e}^K$ and using integration by parts for the above equation, we have

$$(k\nabla\phi_{\chi_e}^K, \nabla\phi_{\chi_e}^K) - \frac{1}{|e|}\int_e \phi_{\chi_e}^K = 0.$$

The Cauchy-Schwarz inequality implies that

$$(k\nabla\phi_{\chi_e}^K, \nabla\phi_{\chi_e}^K) = \frac{1}{|e|}\int_e \phi_{\chi_e}^K \leq |e|^{-\frac{1}{2}}\|\phi_{\chi_e}^K\|_{0,e}. \tag{4.17}$$

Applying the trace theorem and scaling argument [12], it follows that

$$|e|^{-\frac{1}{2}}\|\phi_{\chi_e}^K\|_{0,e} \leq C|e|^{-\frac{1}{2}} h_K^{\frac{1}{2}}\|\nabla\phi_{\chi_e}^K\|_{0,K} \leq C|e|^{-\frac{1}{2}} h_K^{\frac{1}{2}}\|\psi_{\chi_e}^K\|_{0,K}, \tag{4.18}$$

Therefore, by (4.17) and (4.18) we have

$$\|\psi_{\chi_e}^K\|_{0,K}^2 \leq C(k\nabla\phi_{\chi_e}^K, \nabla\phi_{\chi_e}^K) \leq C|e|^{-\frac{1}{2}} h_K^{\frac{1}{2}}\|\psi_{\chi_e}^K\|_{0,K}.$$

This completes the proof. ∎

We define the homogenization equation of the basis equation (3.1) by

$$\begin{cases} \psi_\chi^{*,K} + k^*\eta_\chi^{*,K} = 0 \\ \eta_\chi^{*,K} - \nabla\phi^{*,K} = 0 \\ \quad div(\psi_\chi^{*,K}) = div\chi^K \quad \text{in} \quad K \\ \quad \psi_\chi^{*,K} \cdot n_{\partial K} = \chi^K \cdot n_{\partial K} \quad \text{on} \quad \partial K\,. \end{cases} \tag{4.19}$$

By Theorem 2.1 and the uniqueness of solution of (4.19), we have

$$\psi_\chi^{*,K} = \chi^K, \quad \eta_\chi^{*,K} = (k^*)^{-1}\chi^K. \tag{4.20}$$

Let $w_\epsilon^K(x)$ be the solution (up to a constant) of the equation

$$\begin{cases} -div(k_\epsilon(x)\nabla w_\epsilon^K) & = div(\mathcal{I}_h^* u^*|_K) \ \text{ in } \ K \\ -k_\epsilon(x)\nabla w_\epsilon^K \cdot n_{\partial K} & = (\mathcal{I}_h^* u^*|_K)\cdot n_{\partial K} \ \text{ on } \ \partial K. \end{cases} \tag{4.21}$$

Then the homogenized equation of (4.21) is

$$\begin{cases} -div(k^*\nabla w^{*,K}) &= div(\mathcal{I}_h^* u^*|_K) \ \text{ in } \ K \\ -k^*\nabla w^{*,K}\cdot n_{\partial K} &= (\mathcal{I}_h^* u^*|_K)\cdot n_{\partial K} \ \text{ on } \ \partial K. \end{cases} \tag{4.22}$$

By a straightforward calculation (ref. [26]), we have the following lemma.

LEMMA 4.8. *Let w_ϵ^K and $w^{*,K}$ be defined in (4.21) and (4.22), respectively. Then*

$$\begin{aligned} -k_\epsilon\nabla w_\epsilon^K &= \mathcal{I}_h u^*|_K \ \ in \ \ K \\ -k^*\nabla w^{*,K} &= \mathcal{I}_h^* u^*|_K \ \ in \ \ K. \end{aligned} \tag{4.23}$$

Moreover, we have

LEMMA 4.9. *Let w_ϵ^K and $w^{*,K}$ be defined in (4.21) and (4.22), respectively. Then*

$$\nabla w_\epsilon^K \in X_{1,h}^l(K), \quad \nabla w^{*,K} \in V_h(K).$$

Proof. It is obvious that

$$-div(k_\epsilon(x)\nabla w_\epsilon^K) = div(\mathcal{I}_h^* u^*|_K) = \big(\sum_{e\subset\partial K}\int_e u^*\cdot n ds (div\chi_e^K)\big),$$

and

$$-k_\epsilon(x)\nabla w_\epsilon^K\cdot n_e = (\mathcal{I}_h^*|_K)u^*\cdot n_e = (\sum_{e_j\subset\partial K}\int_{e_j} u^*\cdot n ds\chi_{e_j}^K)\cdot n_e = (\int_e u^*\cdot n ds)\chi_e^K\cdot n_e.$$

By Theorem 2.1 and equation (3.1), it follows

$$\nabla w_\epsilon^K = \sum_{e\subset\partial K}\big((\int_e u^*\cdot n ds)\eta_{\chi_e}^K\big).$$

Similarly, we can show that by (4.20)

$$\nabla w^{*,K} = (k^*)^{-1}\sum_{e\subset\partial K}\big((\int_e u^*\cdot n ds)\chi_e^K\big).$$

This completes the proof. □

For the relationship between p_ϵ and w_ϵ^K, we have the following lemma.

LEMMA 4.10. *Let w_ϵ^K be defined in (4.21). Then*

$$|p_\epsilon - w_\epsilon^K|_{1,K} \le C(\epsilon + h + \sqrt{\epsilon h})\|p^*\|_{2,K} + C\sqrt{\epsilon h^{d-1}}\|p^*\|_{1,\infty,K}. \tag{4.24}$$

The proof of Lemma 4.10 can be obtained by using Lemma 4.8 and the proof of Theorem 3.1 in [14].

We have the following convergence theorem on the periodic case.

THEOREM 4.11. *Let $\big((\theta_\epsilon,u_\epsilon),p_\epsilon\big)$ be the solution of (2.3) and $(\theta_h^l,u_h^l),p_h^l,\lambda_h^l)$ be the solution of (3.5). Then*

$$\begin{aligned} &\|\big((\theta_\epsilon,u_\epsilon),p_\epsilon\big) - \big((\theta_h^l,u_h^l),p_h^l\big)\|_{X\times Q} + \|\mathcal{P}_\partial p_\epsilon - \lambda_h^l\|_{-\frac{1}{2},h} \\ &\le Ch\|f\|_{1,\Omega} + C(\epsilon + h + \sqrt{\epsilon h})\|p^*\|_{2,\Omega} + C\sqrt{\frac{\epsilon}{h}}\|p^*\|_{1,\infty,\Omega}. \end{aligned} \tag{4.25}$$

Proof. By Theorem 4.4, we can use problem (3.3) to perform an error analysis for $\big((\theta_h^l, u_h^l), p_h^l\big)$. Due to Theorem 4.2, it suffices to choose $\big((\xi_h, v_h), q_h)\big) \in X_h^l \times Q_h$ such that the right-hand side of (4.8) is small.

Set $q_h = \mathcal{P}_h p_\epsilon$, the L^2 projection of p_ϵ onto Q_h. Then Poincaré-Friedrichs inequality implies

$$\|p_\epsilon - q_h\|_{0,\Omega} \leq Ch|p_\epsilon|_{1,\Omega}. \tag{4.26}$$

We choose $\xi_h|_K = \nabla w_\epsilon^K$, and the $\xi_h \in X_{1,h}^l$ by Lemma 4.9. Due to Lemma 4.10,

$$\|\theta_\epsilon - \xi_h\|_{0,\Omega} = \big(\sum_K |p_\epsilon - w_\epsilon^K|_{1,K}^2\big)^{\frac{1}{2}} \leq C(\epsilon + h + \sqrt{\epsilon h})\|p^*\|_{2,\Omega} + C\sqrt{\frac{\epsilon}{h}}\|p^*\|_{1,\infty,\Omega}. \tag{4.27}$$

Let $v_h := \mathcal{I}_h u^*$. Note that $div(\mathcal{I}_h u^*)|_K = \langle f \rangle_K$, the integral average of f over K. Then

$$\|div(u_\epsilon - v_h)\|_{0,\Omega} = \big(\sum_K \|f - \langle f\rangle_K\|_{0,K}^2\big)^{\frac{1}{2}} \leq Ch|f|_{1,\Omega}. \tag{4.28}$$

Moreover, by Lemma 4.8 and (4.24)

$$\begin{aligned} \|u_\epsilon - v_h\|_{0,K} &= \|k_\epsilon \nabla p_\epsilon - k_\epsilon \nabla w_\epsilon^K|_{0,K} \\ &\leq C(\epsilon + h + \sqrt{\epsilon h})\|p^*\|_{2,K} + C\sqrt{\epsilon h^{d-1}}\|p^*\|_{1,\infty,K}. \end{aligned} \tag{4.29}$$

Consequently, it follows immediately that

$$\|u_\epsilon - v_h\|_{0,\Omega} \leq C(\epsilon + h + \sqrt{\epsilon h})\|p^*\|_{2,\Omega} + C\sqrt{\frac{\epsilon}{h}}\|p^*\|_{1,\infty,\Omega}. \tag{4.30}$$

Combining (4.26), (4.27), (4.28) and (4.30), it follows

$$\|\big((\theta_\epsilon, u_\epsilon), p_\epsilon\big) - \big((\theta_h^l, u_h^l), p_h^l\big)\|_{X\times Q} \leq Ch\|f\|_{1,\Omega} + C(\epsilon + h + \sqrt{\epsilon h})\|p^*\|_{2,\Omega} + C\sqrt{\frac{\epsilon}{h}}\|p^*\|_{1,\infty,\Omega}. \tag{4.31}$$

Next we employ the technique used in [8] to estimate $\|\mathcal{P}_\partial p_\epsilon - \lambda_h^l\|_{-\frac{1}{2},h}$. Let $\tilde{\tau}_h := |e|(\mathcal{P}_\partial p_\epsilon - \lambda_h^l)\psi_{\chi_e}^K \in \tilde{X}_{2,h}^l(K)$. Then

$$\tilde{\tau}_h \cdot n_e = \mathcal{P}_\partial p_\epsilon - \lambda_h^l \quad \text{on } e \text{ and 0 otherwise.}$$

By (4.16), it follows

$$\|\tilde{\tau}_h\|_{0,K} + h_K\|div\tilde{\tau}_h\|_{0,K} \leq Ch_K^{\frac{1}{2}}\|\mathcal{P}_\partial p_\epsilon - \lambda_h^l\|_{0,e}. \tag{4.32}$$

Define $\tau_h = \tilde{\tau}_h$ in K and $\tau_h = 0$ in $\Omega\backslash$ K. By the second equation in (3.5), we have

$$(\theta_h^l, \tilde{\tau}_h)_K + (p_h^l, div\tilde{\tau}_h)_K = (\mathcal{P}_\partial p_\epsilon - \lambda_h^l, \lambda_h^l)_e. \tag{4.33}$$

Since $\theta_\epsilon = \nabla p_\epsilon$, Green's formula gives

$$(\theta_\epsilon, \tilde{\tau}_h)_K + (p_\epsilon, div\tilde{\tau}_h)_K = (\mathcal{P}_\partial p_\epsilon - \lambda_h^l, p_\epsilon)_e. \tag{4.34}$$

By using (4.33), (4.34) and (4.32), we get

$$\begin{aligned}
&\|\mathcal{P}_\partial p_\epsilon - \lambda_h^l\|_{0,e}^2 = (\mathcal{P}_\partial p_\epsilon - \lambda_h^l, \mathcal{P}_\partial p_\epsilon - \lambda_h^l)_e = (p_\epsilon - \lambda_h^l, \mathcal{P}_\partial p_\epsilon - \lambda_h^l)_e \\
&= (\theta_\epsilon - \theta_h^l, \tilde{\tau}_h)_K + (p_\epsilon - p_h^l, div\tilde{\tau}_h)_K \\
&\leq \|\theta_\epsilon - \theta_h^l\|_{0,K}\|\tilde{\tau}_h\|_{0,K} + \|p_\epsilon - p_h^l\|_{0,K}\|div\tilde{\tau}_h\|_{0,K} \\
&\leq C\big(h^{-\frac{1}{2}}\|p_\epsilon - p_h^l\|_{0,K} + h^{\frac{1}{2}}\|\theta_\epsilon - \theta_h^l\|_{0,K}\big)\|\mathcal{P}_\partial p_\epsilon - \lambda_h^l\|_{0,e},
\end{aligned} \tag{4.35}$$

which gives

$$\|\mathcal{P}_\partial p_\epsilon - \lambda_h^l\|_{0,e} \leq C\big(h^{-\frac{1}{2}}\|p_\epsilon - p_h^l\|_{0,K} + h^{\frac{1}{2}}\|\theta_\epsilon - \theta_h^l\|_{0,K}\big).$$

Consequently,

$$\begin{aligned}
&\|\mathcal{P}_\partial p_\epsilon - \lambda_h^l\|_{-\frac{1}{2},h}^2 = \sum_{K\in\mathfrak{T}}\sum_{e\subset\partial K} h_K\|\mathcal{P}_\partial p_\epsilon - \lambda_h^l\|_{0,e}^2 \\
&\leq C\big(\sum_K h_K^{-1}h_K\|p_\epsilon - p_h^l\|_{0,K}^2 + \sum_K h_K^2\|\theta_\epsilon - \theta_h^l\|_{0,K}^2\big) \\
&\leq C\|p_\epsilon - p_h^l\|_{0,\Omega}^2 + Ch^2\|\theta_\epsilon - \theta_h^l\|_{0,\Omega}^2.
\end{aligned} \tag{4.36}$$

Owing to Theorem 4.6 in [20], we have

$$\|p_\epsilon - p_h^l\|_{0,\Omega} \leq C\big\{\|(\theta_\epsilon, u_\epsilon) - (\theta_h^l, u_h^l)\|_X + \inf_{q_h\in Q_h}\|p_\epsilon - q_h\|_{0,\Omega}\big\}. \tag{4.37}$$

Combining (4.36), (4.37) and (4.31) gives

$$\|\mathcal{P}_\partial p_\epsilon - \lambda_h^l\|_{-\frac{1}{2},h} \leq Ch\|f\|_{1,\Omega} + C(\epsilon + h + \sqrt{\epsilon h})\|p^*\|_{2,\Omega} + C\sqrt{\frac{\epsilon}{h}}\|p^*\|_{1,\infty,\Omega} \tag{4.38}$$

This completes the proof. □

COROLLARY 4.12. *Let $(\theta_\epsilon, u_\epsilon)$ be the solution of (2.3) and (θ_h^l, u_h^l) be the solution of (3.3). Then*

$$\|(\theta_\epsilon, u_\epsilon) - (\theta_h^l, u_h^l)\|_X \leq Ch|f|_{1,\Omega} + C(\epsilon + h + \sqrt{\epsilon h})\|p^*\|_{2,\Omega} + C\sqrt{\frac{\epsilon}{h}}\|p^*\|_{1,\infty,\Omega}$$

Proof. Due to Theorem 4.5 in [20], it follows that

$$\|(\theta_\epsilon, u_\epsilon) - (\theta_h^l, u_h^l)\|_X \leq C\big\{\inf_{(\xi_h, v_h)\in X_h^l}\|(\theta_\epsilon, u_\epsilon) - (\xi_h, v_h)\|_X\big\}.$$

Then using the proof of (4.25) completes the proof immediately. □

4.3.2. Analysis of expanded mixed MsFEM using oversampling techniques. By Theorem 4.11, the local expanded mixed MsFEM without using oversampling techniques causes a resonance error $O(\sqrt{\frac{\epsilon}{h}})$. By oversampling technique, the resonance error $O(\sqrt{\frac{\epsilon}{h}})$ in Theorem (4.11) will reduce to $O(\frac{\epsilon}{h})$. In this subsection we sketch the analysis for the oversampling expanded mixed MsFEM.

Let $S \supset K$ be the local domain described in equation (3.6). We assume that $dist(\partial K, \partial S) \approx h_K$ for the analysis. Let constant c_{jl} be defined in (3.8). The constants

c_{jl} allow us to introduce an extension operator E^S to S from K, e.g., $E^S : V_h(K) \longrightarrow V_h(S)$ is defined by

$$E^S(\sum_j \beta_j \chi_j^K) := \sum_j \sum_l \beta_j c_{jl} \chi_l^S.$$

Similarly, $E^S : \tilde{X}_{2,h}^{os}(K) \longrightarrow X_{2,h}^{l}(S)$ is defined by

$$E^S(\sum_j \beta_j \bar{\psi}_{\chi_j}^K) := \sum_j \sum_l \beta_j c_{jl} \psi_{\chi_l}^S.$$

Since $dist(\partial K, \partial S) \approx h_K$, the extension operator E^S has the property

$$\|E^S(v^K)\|_{0,S} \approx \|v^K\|_{0,K}, \quad \text{for} \quad \forall v^K \in V_h(K) \quad \text{or} \quad \tilde{X}_{2,h}^{os}(K).$$

In order to analyze convergence, we define $w_\epsilon^S(x)$ be the solution (up to a constant) of the following equation

$$\begin{cases} -div(k_\epsilon(x)\nabla w_\epsilon^S) & = div(E^S(\mathcal{I}_h^* u^*|_K)) \ \text{ in } \ S \\ -k_\epsilon(x)\nabla w_\epsilon^S \cdot n_{\partial S} & = E^S(\mathcal{I}_h^* u^*|_K) \cdot n_{\partial S} \ \text{ on } \ \partial S. \end{cases} \tag{4.39}$$

Here we note that $\mathcal{I}_h^* u^*|_K$ is the local interpolation on $V_h(K)$ (i.e., $RT_0(K)$). We define the multiscale interpolation operator $\mathcal{I}_h^{os} : [H^1(\Omega)]^d \longrightarrow \tilde{X}_{2,h}^{os}$ for velocity by

$$\mathcal{I}_h^{os}(v) := \sum_{e \in \mathcal{F}_h} (\int_e v \cdot n_e ds) \bar{\psi}_{\chi_e}.$$

Then by using a procedure similar to Lemma 4.8, Lemma 4.9 and straightforward calculations, we obtain the following lemma.

LEMMA 4.13. *Let w_ϵ^S be defined in (4.39). Then*

$$-k_\epsilon \nabla w_\epsilon^S = E^S(\mathcal{I}_h^{os} u^*|_K) \ \ on \ \ S, \quad -k_\epsilon \nabla w_\epsilon^S|_K = \mathcal{I}_h^{os} u^*|_K \ \ on \ \ K. \tag{4.40}$$

Moreover, $\nabla w_\epsilon^S|_K = \sum_{e \subset \partial K} (\int_e u^* \cdot n_e ds) \bar{\eta}_{\chi_e}^K \in X_{1,h}^{os}(K)$, where $\bar{\eta}_{\chi_e}^K$ is defined in (3.7).

We have the convergence result for the oversampling expanded mixed MsFEM.

THEOREM 4.14. *Let $((\theta_\epsilon, u_\epsilon), p_\epsilon)$ be the solution of (2.3) and $(\theta_h^{os}, u_h^{os}, p_h^{os}, \lambda_h^{os})$ be the solution of (3.11). Then*

$$\begin{aligned} &\sum_K \|\big((\theta_\epsilon, u_\epsilon), p_\epsilon\big) - \big((\theta_h^{os}, u_h^{os}), p_h^{os}\big)\|_{X(K)\times Q(K)} + \|\mathcal{P}_\partial p_\epsilon - \lambda_h^{os}\|_{-\frac{1}{2},h} \\ &\leq C(h+\epsilon)(\|f\|_{1,\Omega} + \|p^*\|_{2,\Omega}) + C(\frac{\epsilon}{h} + \sqrt{\epsilon})(\|p^*\|_{1,\infty,\Omega} + \|f\|_{0,\Omega}). \end{aligned} \tag{4.41}$$

The proof of Theorem 4.14 is presented in Appendix A.

4.4. Error analysis in G convergence. In subsection 4.3, we have investigated the case when k_ϵ in (2.1) is ϵ periodic. However, the expanded mixed MsFEMs can also be applied to non-periodic separable scales. In this section we will discuss the convergence for the case of separable scales described in $G-$convergence (ref. [27]). $G-$convergence is more general than the periodic homogenization described in Subsection 4.3.

A sequence of matrices k_ϵ is $G-$convergent to k^* if for any open set $\omega \subset \Omega$ and any right-hand side $f \in H^{-1}(\omega)$ in (2.1), if the sequence of the solutions p_ϵ in (2.1) satisfies

$$p_\epsilon \rightharpoonup p^* \ \text{ weakly in } \ H^1(\omega) \ \text{ as } \ \epsilon \to 0,$$

where p^* is the solution of the equation (4.15), in which k^* is the homogenized matrix in the sense of $G-$convergence. The $G-$convergence implies that

$$k_\epsilon \nabla p_\epsilon \rightharpoonup k^* \nabla p^* \ \text{ weakly in } \ L^2(\omega) \ \text{ as } \ \epsilon \to 0.$$

There is no explicit formula for the matrix k^*, which is defined as a limit in the distributional sense, i.e.,

$$k_\epsilon \nabla \mathcal{N}_\epsilon^i \rightharpoonup k^* e_i \ \text{ in } \ \mathcal{D}'(\omega; \mathbb{R}^d),$$

where the auxiliary functions $\mathcal{N}_\epsilon^i$ $(i = 1, \cdots, d)$ satisfy

$$\mathcal{N}_\epsilon^i \rightharpoonup x_i \ \text{ weakly in } \ H^1(\omega) \ \text{ as } \ \epsilon \to 0.$$

The auxiliary functions are not explicit. We define the corrector matrix $\nabla \mathcal{N}_\epsilon = (\frac{\partial \mathcal{N}_\epsilon^i}{\partial x_j})_{i,j=1,\cdots,d}$.

The following lemma is about corrector in $G-$convergence.

LEMMA 4.15. *[29] Let k_ϵ be a sequence $G-$converging to k^* as $\epsilon \to 0$. Then*

$$\nabla p_\epsilon = \nabla \mathcal{N}_\epsilon \cdot \nabla p^* + R_\epsilon^\omega,$$

where $R_\epsilon^\omega \to 0$ strongly in $L^1(\omega)$ as $\epsilon \to 0$. Moreover, if $\nabla \mathcal{N}_\epsilon$ is bounded in $L^r(\omega)$ for some r such that $2 \le r \le \infty$, and $\nabla p^* \in L^s(\omega)$ for some s such that $2 \le s < \infty$, then $R_\epsilon^\omega \to 0$ strongly in $L^t(\omega)$, as $\epsilon \to 0$, where $t = \min\{2, \frac{rs}{r+s}\}$. We have the following convergence theorem for the case of $G-$convergence.

THEOREM 4.16. *Let $\big((\theta_\epsilon, u_\epsilon), p_\epsilon\big)$ be the solution of (2.3) and $(\theta_h^l, u_h^l, p_h^l, \lambda_h^l)$ be the solution of (3.5). If $\nabla \mathcal{N}_\epsilon \in L^\infty(K)$ for all K, then*

$$\begin{aligned} &\lim_{\epsilon \to 0} \big\{ \|\big((\theta_\epsilon, u_\epsilon), p_\epsilon\big) - \big((\theta_h^l, u_h^l), p_h^l\big)\|_{X \times Q} + \|\mathcal{P}_\partial p_\epsilon - \lambda_h^l\|_{-\frac{1}{2},h} \big\} \\ &\le Ch(|u^*|_{0,\Omega} + \|f\|_{1,\Omega}). \end{aligned} \tag{4.42}$$

Proof. The proof of (4.42) is similar to the proof of (4.25). We set $q_h = \mathcal{P}_h p_\epsilon$, $\xi_h|_K = \nabla w_\epsilon^K$ and $v_h = \mathcal{I}_h u^*$ and then use Theorem 4.2. By the proof of (4.25), it immediately follows

$$\|div(u_\epsilon - v_h)\|_{0,\Omega} + \|p_\epsilon - q_h\|_{0,\Omega} \le Ch(|p_\epsilon|_{1,\Omega} + |f|_{1,\Omega}) \le Ch\|f\|_{1,\Omega}. \tag{4.43}$$

By Lemma 4.8 and Lemma 4.15

$$\begin{aligned} &\|\nabla p_\epsilon - \nabla w_\epsilon^K\|_{0,K} \\ &\le \|\nabla p_\epsilon - \nabla \mathcal{N}_\epsilon \nabla p^*\|_{0,K} + \|\nabla \mathcal{N}_\epsilon(\nabla p^* - \nabla w^{*,K})\|_{0,K} + \|\nabla \mathcal{N}_\epsilon \nabla w^{*,K} - \nabla w_\epsilon^K\|_{0,K} \\ &\le \|\nabla p_\epsilon - \nabla \mathcal{N}_\epsilon \nabla p^*\|_{0,K} + \|\nabla \mathcal{N}_\epsilon\big((k^*)^{-1}(u^* - \mathcal{I}_h^* u^*)\big)\|_{0,K} + \|R_\epsilon^K\|_{0,K} \\ &\le \|\nabla p_\epsilon - \nabla \mathcal{N}_\epsilon \nabla p^*\|_{0,K} + Ch|u^*|_{0,K} + \|R_\epsilon^K\|_{0,K}, \end{aligned} \tag{4.44}$$

which gives

$$\|\nabla p_\epsilon - \nabla \xi_h\|_{0,\Omega} \leq C\|R_\epsilon^\Omega\|_{0,\Omega} + Ch|u^*|_{0,\Omega} + C\sum_K \|R_\epsilon^K\|_{0,K}. \tag{4.45}$$

Similarly we have

$$\|u_\epsilon - v_h\|_{0,\Omega} \leq C\|R_\epsilon^\Omega\|_{0,\Omega} + Ch|u^*|_{0,\Omega} + C\sum_K \|R_\epsilon^K\|_{0,K}. \tag{4.46}$$

By combining (4.43), (4.45), (4.46) and Lemma 4.15 and letting $\epsilon \to 0$, we have

$$\lim_{\epsilon\to 0} \|\big((\theta_\epsilon, u_\epsilon), p_\epsilon\big) - \big((\theta_h^l, u_h^l), p_h^l\big)\|_{X\times Q} \leq Ch(|u^*|_{0,\Omega} + \|f\|_{1,\Omega}). \tag{4.47}$$

By following the proof of Theorem 4.11 and using (4.47), we can immediately obtain that

$$\lim_{\epsilon\to 0} \|\mathcal{P}_\partial p_\epsilon - \lambda_h^l\|_{-\frac{1}{2},h} \leq Ch(|u^*|_{0,\Omega} + \|f\|_{1,\Omega}). \tag{4.48}$$

The proof of (4.42) is completed by combining (4.47) and (4.48). ∎

Because no explicit formula is available for homogenization matrix k^*, we are not able to obtain an explicit convergence rate in $G-$convergence. The approximation rate is only presented in terms of limit as $\epsilon \to 0$. We can also obtain the convergence of oversampling expanded mixed MsFEM in terms of $G-$convergence, and the convergence result is the same as in Theorem 4.16.

4.5. Error analysis for global expanded mixed MsFEM. In this subsection, we present the convergence results for the expanded mixed MsFEM using global information. We consider the continuum scales for the global expanded mixed MsFEM.

For analysis, we make the following assumption for global information.

ASSUMPTION 4.1. *There exist global fields* $\{u_1, \cdots, u_N\}$ *and continuous functions* $A_i(x)$ $(i = 1, \cdots N)$ *such that*

$$u = \sum_{i=1}^N A_i(x)u_i, \quad A_i(x) \in C^\alpha.$$

The existence of these global fields has been discussed in the literature recently (see e.g., [1, 10, 26, 30]). In particular, Owhadi and Zhang [30] develop global fields $(u_1, \ldots, u_d)$ that are solutions of the following equations

$$\begin{cases} u_i + k\theta_i = 0 \ \text{ in } \ \Omega \\ \theta_i - \nabla p_i = 0 \ \text{ in } \ \Omega \\ div(u_i) = 0 \ \text{ in } \ \Omega \\ p_i = x_i \ \text{ on } \ \partial\Omega\,, \end{cases} \tag{4.49}$$

where $x = (x_1, \ldots, x_d)$. Using these global fields, and Theorem 1.3 in [30], we can prove the following proposition.

PROPOSITION 4.17. *Let* (θ, u) *be the solution of (2.2) and* (θ_i, u_i, p_i) *solve equation (4.49) for* $i = 1, \ldots, d$. *Let* $\mathbb{P} = (p_1, \ldots, p_d)$. *If* $(\nabla\mathbb{P})^T k \nabla\mathbb{P}$ *satisfies the anisotropic condition described in Theorem 1.3 in [30], then*

$$u = \sum_{i=1}^d A_i(x)u_i, \quad \theta = \sum_{i=1}^d A_i(x)\theta_i,$$

where $A_i(x)$ are continuous functions. Moreover, for any $s > d$, $i = 1, \ldots, d$,

$$\|A_i\|^2_{C^{1-\frac{d}{s}}(\Omega)} \leq C\|f\|^2_{0,s,\Omega},$$

where the constant C depends on the anisotropic condition and s.

REMARK 4.1. *To simplify computation of global fields and the coupled coarse-scale system by expanded mixed MsFEMs, we may use a single global field ($N = 1$) to construct the basis functions. This simplification has been shown to be effective for relevant two-phase flow simulations [1, 26].*

Let $\mathcal{I}_h^g u$ be the interpolation of u, with its restriction on K defined by

$$\mathcal{I}_h^g u|_K = \sum_{i=1}^{N} \sum_{e \subset \partial K} \Big(\int_e A_i u_i \cdot n_e ds\Big)\psi^K_{i,\chi_e},$$

where the velocity basis function ψ^K_{i,χ_e} is defined in (3.12). Then it follows that

$$(div(u - \mathcal{I}_h^g u), q_h) = 0 \quad \text{for} \quad \forall q_h \in Q_h.$$

By Theorem 3.4 in [1], there exists $0 < \mu \leq 1$, which depends on α and d, such that

$$\|u - \mathcal{I}_h^g u\|_{0,\Omega} \leq Ch^\mu \Big(\sum_i \|A_i\|_{C^\alpha(\Omega)}\Big). \tag{4.50}$$

Let $w(x)$ be the solution (up to a constant) of the following equation

$$\begin{cases} -div(k\nabla w) & = div(\mathcal{I}_h^g u|_K) \ \text{ in } \ K \\ -k\nabla w \cdot n_{\partial K} & = (\mathcal{I}_h^g u|_K) \cdot n_{\partial K} \ \text{ on } \ \partial K. \end{cases} \tag{4.51}$$

Then we have the following lemma.

LEMMA 4.18. *Let w be solution of (4.51). Then*

$$-k(x)\nabla w = \mathcal{I}_h^g u|_K \quad \text{on } K.$$

Moreover, $\nabla w \in X^g_{1,h}(K)$.

The proof of Lemma 4.18 is given in Appendix B. By using Lemma 4.18, the interpolation estimate (4.50) and the techniques in the proof of Theorem 4.11, we can derive the convergence result for the global expanded mixed MsFEM.

THEOREM 4.19. *Let $\big((\theta_\epsilon, u_\epsilon), p_\epsilon\big)$ be the solution of (2.3) and $(\theta_h^g, u_h^g, p_h^g, \lambda_h^g)$ be the solution of (3.14). Under Assumption 4.1, there exists μ ($0 < \mu \leq 1$) such that*

$$\|\big((\theta, u), p\big) - \big((\theta_h^g, u_h^g), p_h^g\big)\|_{X\times Q} + \|\mathcal{P}_\partial p - \lambda_h^g\|_{-\frac{1}{2},h} \leq Ch^\mu, \tag{4.52}$$

where $C = C(\|f\|_{1,\Omega})$.

Theorem 4.19 shows that the convergence of global expanded mixed MsFEM is independent of small scales, and the resonance error is removed using the global information.

5. Numerical results. In this section, we present numerical results that highlight the advantages of the proposed expanded mixed MsFEMs. In particular, we show the improvement in the accuracy of the gradient unknown θ and the velocity unknown u obtained with this new family of methods. In addition, we confirm that if the media has strong non-local features (e.g., channels and fractures), then the use

of global information in the construction of the basis functions significantly improves the accuracy of the multiscale solution

In all of the numerical experiments reported below, we use RT_0 in three dimensions, both as the fine-scale velocity space and as fine-scale shape functions for the space approximating ∇p in $L^2(\Omega)^3$ (not conforming in $H(div, \Omega)$) . The domain Ω is discretized by a uniform hexahedral fine mesh of size h and a uniform hexahedral coarse mesh of size $H > h$. The fine mesh is nested in the coarse mesh. The reference solutions for pressure, velocity, and ∇p are computed by solving the fine-scale expanded MFEM.

Our primary focus in this section is on the behavior of the error of the MsFEM solutions for the velocity and pressure gradient. These errors are significantly affected by features of the multiscale models and by the different boundary conditions that are used in the construction of the multiscale basis functions. The velocity is particularly important and required for multi-phase simulations. All errors reported in this section are measured in L^2. We are also interested in the practical application of simulating multi-phase flow. Therefore, in addition to velocity error data, we present solutions obtained by the IMPES (implicit pressure, explicit saturation) method for the coupled saturation and pressure equations of two-phase flow (incompressible and immiscible).

5.1. Low permeability channel. In the first experiment, the domain Ω is the unit cube. We take $h = 1/24$ and $H = 1/8$, so that each coarse element contains $3 \times 3 \times 3$ fine elements. The source function is as follows:

$$f(x, y, z) = \begin{cases} 1 & \text{if } (x, y, z) \text{ is in } (0, H)^3, \\ -1 & \text{if } (x, y, z) \text{ is in } (1 - H, 1)^3, \\ 0 & \text{otherwise.} \end{cases} \tag{5.1}$$

This source function represents injection and production wells in opposite corners of the domain, occupying coarse elements. It is a practical example that demonstrates corner to corner flow across the domain, allowing us to test different numerical methods in simulating flow for various permeability fields.

In the case that the permeability is positive and bounded well above zero everywhere, the expanded mixed MsFEM gives comparable (almost identical) results to the standard mixed MsFEM. However, if the permeability is not positive everywhere, the standard mixed MsFEM is not applicable. Moreover, if the permeability is not bounded well above zero everywhere, the finite precision may significantly degrade the its performance. Table 5.1 demonstrates this fact, where a test is reported using a channel of low permeability. This model problem does not have well separated scales. The channel has one fine cell's width in the $y-$ and $z-$directions, and it extends across the entire domain in the $x-$direction. More specifically, the channel occupies $(0, 1) \times (\frac{4}{24}, \frac{5}{24}) \times (\frac{7}{24}, \frac{8}{24})$. Inside the channel, $k = 10^{-4}$, and elsewhere $k = 1$.

The label "MsFEM" in Table 5.1 represents the standard mixed MsFEM, with variables for pressure and velocity only. This method makes no direct approximation of the pressure gradient, but we approximate ∇p with velocity divided by permeability, when the permeability is positive everywhere. "Expanded MsFEM" is the expanded mixed MsFEM, which approximates the pressure gradient ∇p locally by non-conforming Raviart-Thomas elements. "GMsFEM" means that global information, specifically the fine-scale velocity obtained from the expanded mixed FEM, was used in constructing the coarse multiscale basis functions. We observe that using global information reduces the error by more than a factor of 20 in both the velocity and the pressure gradient, while the difference between standard MsFEM and

TABLE 5.1
Low permeability channel

	MsFEM	GMsFEM	Expanded MsFEM	Expanded GMsFEM
Velocity error	1.173×10^{-3}	5.005×10^{-5}	1.173×10^{-3}	5.005×10^{-5}
Velocity norm	5.649×10^{-3}	5.649×10^{-3}	5.649×10^{-3}	5.649×10^{-3}
∇p error	1.739×10^{-3}	5.284×10^{-5}	1.858×10^{-3}	5.7812×10^{-5}
∇p norm	5.670×10^{-3}	5.670×10^{-3}	5.670×10^{-3}	5.670×10^{-3}

TABLE 5.2
Channel with vanishing permeability

	Expanded MsFEM	Expanded GMsFEM
Velocity error	1.140×10^{-3}	1.122×10^{-4}
Velocity norm	5.642×10^{-3}	5.642×10^{-3}
∇p error	1.461×10^{-3}	9.338×10^{-4}
∇p norm	5.782×10^{-3}	5.782×10^{-3}

expanded MsFEM is negligible. In the remainder of this section, we do not report results for standard MsFEM.

Next, we test the more interesting case of a permeability that vanishes in the channel. Standard mixed MsFEMs cannot be used in this case. In each cell within the channel, we define the permeability to be the vanishing, non-negative function

$$k = \max(0, 1 - 32x(1-x)y(1-y)), \qquad \text{for } (x,y) \in (0,1)^2, \tag{5.2}$$

defined on the reference unit square (see Figure 5.1 for the contour plot). Outside the channel, $k = 1$. This permeability has no scale separation, and it ensures a positive definite mass matrix (weighted by k) for the discontinuous space approximating ∇p in $L^2(\Omega)^3$. Note that expanded mixed MsFEMs allow the permeability to vanish locally within fine cells, unlike standard mixed MsFEMs which involve k^{-1}, but the mass matrix weighted by k must be invertible. The results for the expanded methods are shown in Table 5.2. Global information reduces the relative velocity error from approximately 20% to 2% and the relative pressure gradient error from approximately 25% to 16%.

5.2. Oscillatory permeability. The next experiment demonstrates the resonance error that appears in the velocity and the pressure gradient that are obtained using the local expanded MsFEM. The permeability is taken to be the oscillatory function

$$k = (\sin(20\pi x) + 1.5)(\sin(20\pi y) + 1.5) \tag{5.3}$$

on the domain $\Omega = (0,1) \times (0,1) \times (0, \frac{1}{8})$, and the mesh has $100 \times 100 \times 8$ fine cells. The source function is the two-dimensional analog of (5.1) (constant in the z-direction), namely

$$f(x,y,z) = \begin{cases} 1 & \text{if } (x,y) \text{ is in } (0,H)^2, \\ -1 & \text{if } (x,y) \text{ is in } (1-H,1)^2, \\ 0 & \text{otherwise.} \end{cases} \tag{5.4}$$

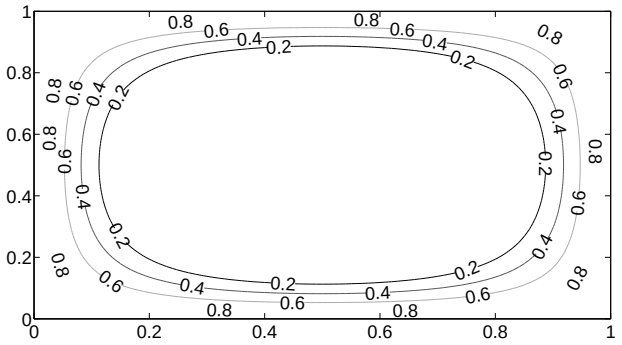

FIG. 5.1. *Partially vanishing permeability within a reference fine cell*

TABLE 5.3
Oscillatory permeability without scale separation, $100 \times 100 \times 8$ *fine mesh*

	$20 \times 20 \times 1$ coarse mesh		$10 \times 10 \times 1$ coarse mesh	
	Exp. MsFEM	Exp. GMsFEM	Exp. MsFEM	Exp. GMsFEM
Velocity error	2.066×10^{-3}	1.050×10^{-4}	1.827×10^{-3}	7.606×10^{-4}
Velocity norm	5.143×10^{-3}	5.143×10^{-3}	5.143×10^{-3}	5.143×10^{-3}
∇p error	1.370×10^{-3}	1.452×10^{-4}	1.552×10^{-3}	5.360×10^{-4}
∇p norm	3.254×10^{-3}	3.254×10^{-3}	3.254×10^{-3}	3.254×10^{-3}

Thus the problem is essentially two-dimensional, although we solve in a three-dimensional domain. The solution will be approximately constant in the z-direction, so we simply plot an x-y slice. We tested both local and global expanded mixed MsFEMs with coarse meshes of size $20 \times 20 \times 1$ (each coarse cell having $5 \times 5 \times 8$ fine cells) and $10 \times 10 \times 1$ (each coarse cell having $10 \times 10 \times 8$ fine cells). In the $20 \times 20 \times 1$ case, the permeability has one period per coarse edge length. Table 5.3 lists the error for both methods on the two choices of coarse grids.

The local expanded mixed MsFEM clearly suffers from the resonance errors in the velocity and the pressure gradient. In this example, refinement of the coarse mesh does not change the error significantly because the oscillations in k are not resolved, even by the $20 \times 20 \times 1$ coarse mesh. In fact, the error of the velocity actually increases slightly when the coarse grid is refined. Figure 5.2 shows the x-component of the reference velocity on the fine grid (top left), and the excellent agreement with the x-component of the velocity obtained with the global expanded mixed MsFEM on the $20 \times 20 \times 1$ coarse grid (top right). In contrast, the impact of the resonance errors on the x-component of the velocity obtained with the local expanded mixed MsFEM is evident in Figure 5.2 for both the $10 \times 10 \times 1$ (bottom-left) and $20 \times 20 \times 1$ (bottom-right) coarse grids. Note that these plots are in an x-y slice, as the solutions are constant in the z-direction. On the other hand, the global expanded mixed MsFEM performs well in this example, and the refinement of the coarse mesh reduces the error by more than half.

5.3. IMPES with random shales. To compare the performance of the local and global expanded mixed MsFEMs for a two-phase flow problem, we use an Im-

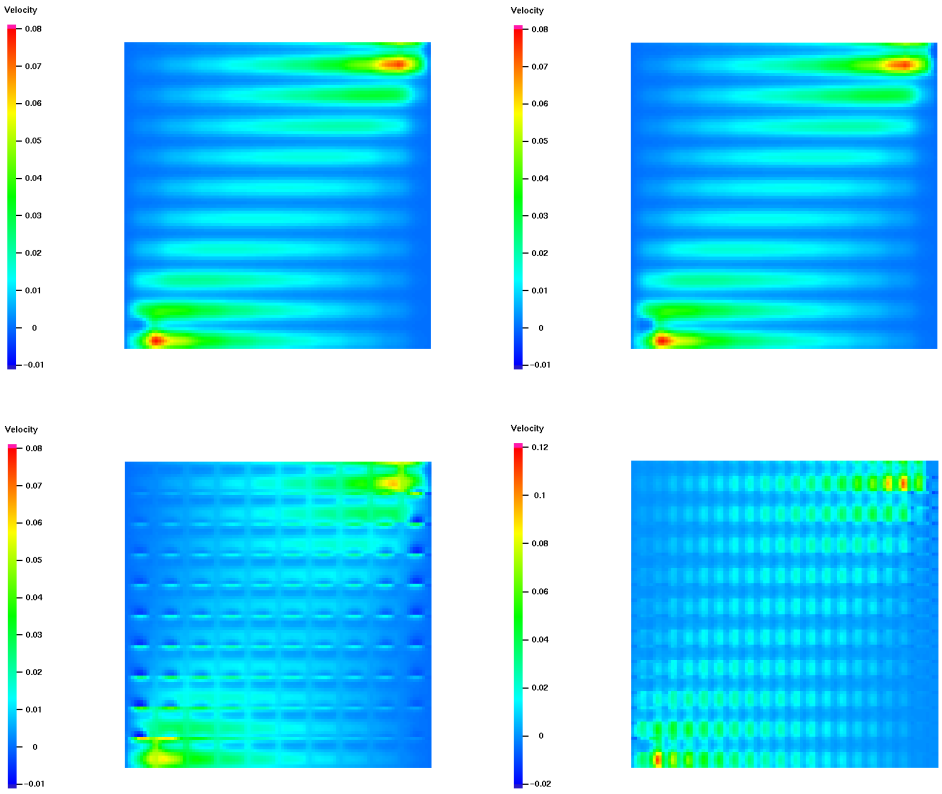

FIG. 5.2. *The x-component of the velocity for the oscillatory permeability field* (5.3) *is plotted for the fine-scale reference solution (top-left), and for three expanded mixed MsFEMs. The solution obtained with the global expanded mixed MsFEM on the* $20 \times 20 \times 1$ *coarse grid (top right) shows excellent agreement with the reference solution. The solutions obtained with the local expanded mixed MsFEM on the* $10 \times 10 \times 1$ *coarse grid (bottom left) and the* $20 \times 20 \times 1$ *coarse grid (bottom right) show the impact of the resonance errors.*

plicit Pressure Explicit Saturation (IMPES) formulation. The boundary conditions that we use to define the global expanded MsFEM basis functions are obtained from the fine-scale expanded MFEM solution at the initial time. We note that in very complex highly varying flows it may be advantageous to update these basis functions by updating the fine-scale expanded MFEM solution that is used in their construction. However, our current study is focused on the effect of the two different velocity approximations, and hence, we fix the multiscale bases throughout the simulation.

The two-phase flow scenario that we consider is the traditional two-spot problem on a square domain (e.g., [1, 25]), in which the water is injected at the bottom left corner and oil is produced at the top right corner. Here, we use simple fixed rate wells that are constant over a coarse cell. We note that it is possible to define a well on a fine cell, and capture the influence of the near-well heterogeneity, by modifying the source term in the construction of the basis functions. Similar modifications were developed to address this issue in the subgrid upscaling method [4] and the standard mixed MsFEM [2]. However, fine-scale wells are beyond the scope of this paper.

This two-spot problem is essentially two dimensional, with the fine-grid discretization having $h = 1/100$ ($100 \times 100 \times 8$ mesh) and $H = 1/10$ or $1/20$. The logarithm of

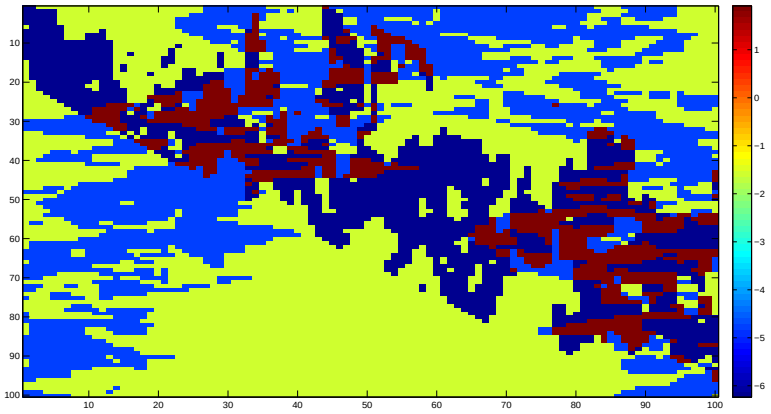

FIG. 5.3. *Logarithm of permeability field used in the two-phase flow two-spot problem.*

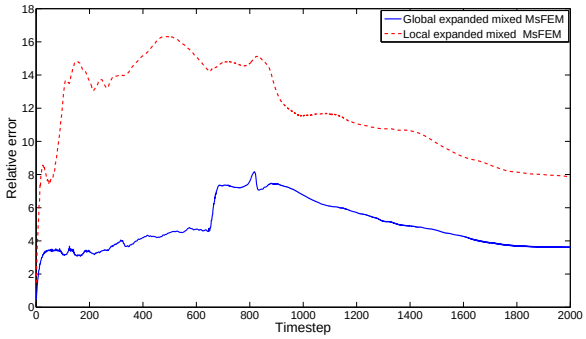

FIG. 5.4. *Relative saturation errors (percentage) at each timestep of the IMPES simulation, for global and local expanded mixed MsFEM*

the permeability field is plotted in Figure 5.3 and includes features that are representative of shale barriers and sandy deposits or channels. Specifically, the darkest blue cells have a permeability of 10^{-6}, but are masked by the vanishing function given in (5.2) on the reference cell to represent a shale barrier. In contrast, the red cells have a permeability of 100 and represent sandy deposits or channels. The remainder of the fine-scale cells are assigned a moderate or low permeability, and are shown as two distinct colors.

The water and oil mobilities are defined simply as the quadratic functions $\lambda_w(S_w) = \frac{S_w^2}{\mu_w}$ and $\lambda_o(S_w) = \frac{(1-S_w)^2}{\mu_o}$, respectively. Here, μ_α denotes the viscosity of phase α, and we take $\mu_w = 0.5$, $\mu_o = 1$. The total mobility $\lambda(S_w) := \lambda_w(S_w) + \lambda_o(S_w)$. Then the pressure equation is given (in the absence of gravity and capillary effects) by

$$-div\big(\lambda(S_w)k\nabla p\big) = q.$$

At each timestep, we use the velocity u computed from the pressure equation to ad-

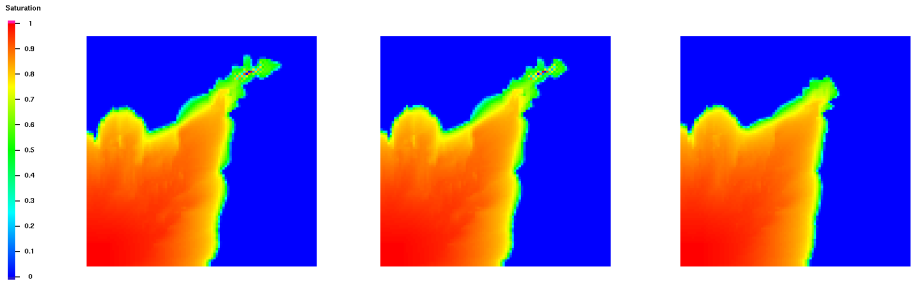

FIG. 5.5. *Water saturation at the 700th timestep computed with the fine-scale reference velocity (left); with the coarse global expanded mixed MsFEM velocity (middle); and with the coarse local expanded mixed MsFEM velocity (right).*

TABLE 5.4
Randomly vanishing permeability without scale separation, $100 \times 100 \times 8$ *fine mesh*

	$20 \times 20 \times 1$ coarse mesh		$10 \times 10 \times 1$ coarse mesh	
	Exp. MsFEM	Exp. GMsFEM	Exp. MsFEM	Exp. GMsFEM
Velocity error	2.184×10^{-3}	5.438×10^{-4}	2.218×10^{-3}	7.137×10^{-4}
Velocity norm	6.202×10^{-3}	6.202×10^{-3}	6.202×10^{-3}	6.202×10^{-3}
∇p error	3.529×10^{-3}	1.999×10^{-3}	3.636×10^{-3}	2.283×10^{-3}
∇p norm	1.471×10^{-2}	1.471×10^{-2}	1.471×10^{-2}	1.471×10^{-2}

vance the water saturation S_w by an explicit discretization of the saturation equation

$$\frac{\partial S_w}{\partial t} + div(f_w(S_w)u) = 0, \qquad \text{with } f_w(S_w) = \frac{\lambda_w(S_w)}{\lambda_w(S_w) + \lambda_o(S_o)}.$$

Figure 5.4 shows a plot of the saturation error in the $L^2(\Omega)$ norm (relative to the reference IMPES saturation computed with the fine-scale expanded mixed FEM velocity), at all 2000 time steps. The water saturation, S_w, at the 700th timestep is plotted in Figure 5.5 by using the fine-scale velocity and the global and local expanded mixed MsFEM velocities. Figure 5.5 shows that the IMPES solution based on the global expanded mixed MsFEM velocity remains close to the reference solution throughout the long simulation, whereas the local expanded mixed MsFEM velocity results in substantial error very early in the simulation. The error naturally decreases later in the simulation, when most of the domain becomes highly saturated with water.

The IMPES experiments discussed above used coarse velocity fields on a $10 \times 10 \times 1$ coarse mesh ($H = 1/10$), with each coarse cell discretized by $10 \times 10 \times 8$ fine cells. To study the coarse velocity error behavior, we also computed the coarse velocity on a $20 \times 20 \times 1$ coarse mesh, with each coarse cell discretized by $5 \times 5 \times 8$ fine cells. The results are reported in Table 5.4. The global expanded mixed MsFEM velocity is about 25% more accurate on the $20 \times 20 \times 1$ coarse mesh than on the $10 \times 10 \times 1$, while the local expanded mixed MsFEM velocity improves by less than 2%. Without global information, non-local effects result in large errors even after refinement.

We conclude that the expanded mixed MsFEM method is very effective in approximating both the pressure gradient and velocity when a locally vanishing permeability field makes standard mixed MsFEM methods infeasible. Practical simulations of two-phase flow demonstrate the high degree of accuracy attained by using global information in constructing the coarse basis functions. Thus the expanded mixed for-

mulation with global information is the most robust and accurate method considered in this study for applications involving a locally vanishing permeability field.

6. Conclusions. We developed a family of expanded mixed MsFEMs for elliptic equations and considered their hybrid formulation. In this formulation, the four unknowns were solved simultaneously, namely, the pressure, gradient of pressure, Lagrange multipliers, and velocity. The expanded mixed MsFEMs work well for the case that the coefficient (e.g., permeability) is very small or locally vanishing in some regions of the domain. This case has important applications in reservoir simulation. In contrast the standard mixed MsFEMs require the coefficient to be uniformly positive everywhere. In addition, expanded mixed MsFEMs provide the gradient of pressure without significantly increasing the computational cost relative to the standard method.

We analyzed the expanded mixed MsFEMs for separable scales and non-separable scales, and established a priori error estimates. We showed that the convergence rates of the local expanded MsFEMs depend on both the small physical scales and on the coarse-mesh size. In contrast, we showed that the global expanded mixed MsFEMs achieves a convergence rate that only depends on the coarse-mesh size. To support this analysis we applied the expanded mixed MsFEMs to various models of flow in heterogeneous porous media. For the models with non-separable spatial scales, significantly better accuracy was achieved by using global information to construct the multiscale basis functions. Moreover, for the periodic example of separable scales using global information eliminated the resonance errors observed in the the local expanded mixed MsFEM. These numerical results showed the efficiency and robustness of the developed methods.

Acknowledgments. We would like to thank the referees for their comments and suggestions to improve the paper.

Appendix A. proof of Theorem 4.14.

Due to Theorem 4.5, problem (3.11) is equivalent to problem (3.10), and we can use problem (3.10) to estimate the errors for $((\theta_h^{os}, u_h^{os}), p_h^{os})$. By the estimate (4.9), we have

$$\begin{aligned}
&\sum_K \|\big((\theta_\epsilon, u_\epsilon), p_\epsilon\big) - \big((\theta_h^{os}, u_h^{os}), p_h^{os}\big)\|_{X(K)\times Q(K)} \\
&\leq C\big\{ \inf_{(\xi_h, v_h, q_h)\in X_{1,h}^{os}\times X_{2,h}^{os}\times Q_h} \sum_K \|((\theta_\epsilon, u_\epsilon), p_\epsilon) - ((\xi_h, v_h), q_h)\|_{X(K)\times Q(K)}\big\} \\
&+ \sum_{v_h\in X_{2,h}^{os}\setminus\{0\}} \frac{-(\theta_\epsilon, v_h) - \sum_K (div(v_h), p_\epsilon)}{\sum_K \|v_h\|_{div,K}} \\
&:= I_1 + I_2.
\end{aligned} \tag{A.1}$$

We set $q_h = \mathcal{P}_h p_\epsilon$, $\xi_h|_K = \nabla w_\epsilon^S|_K$ and $v_h = \mathcal{I}_h^{os} u^*$ in (A.1). Lemma 4.13 shows that $\xi_h \in X_{1,h}^{os}$ and $v_h \in X_{2,h}^{os}$. By the Lemma 4.6 in [14], we obtain

$$|I_1| \leq C(h+\epsilon)(\|f\|_{1,\Omega} + \|p^*\|_{2,\Omega}) + C(\frac{\epsilon}{h} + \sqrt{\epsilon})\|p^*\|_{1,\infty,\Omega}. \tag{A.2}$$

By using the proof of Theorem 2.2 in [14], we estimate the consistence error I_2 by

$$|I_2| \leq C(h+\epsilon)(\|f\|_{1,\Omega} + \|p^*\|_{2,\Omega}) + C(\frac{\epsilon}{h} + \sqrt{\epsilon})(\|p^*\|_{1,\infty,\Omega} + \|f\|_{0,\Omega}). \tag{A.3}$$

Next we estimate $\|\mathcal{P}_\partial p_\epsilon - \lambda_h^{os}\|_{-\frac{1}{2},h}$. Let $\tilde{\tau}_h := |e|(\mathcal{P}_\partial p_\epsilon - \lambda_h^{os})\bar{\psi}_{\chi_e}^K \in \tilde{X}_{2,h}^{os}(K)$ and the operator $\mathcal{M}_h$ be defined in (3.9). Then

$$\mathcal{M}_h(\tilde{\tau}_h)\cdot n_e = \mathcal{P}_\partial p_\epsilon - \lambda_h^{os} \quad \text{on } e \text{ and 0 otherwise.}$$

By direct calculation or scaling argument, it follows

$$\|\mathcal{M}_h(\tilde{\tau}_h)\|_{0,K} + h_K\|div\mathcal{M}_h(\tilde{\tau}_h)\|_{0,K} \le Ch_K^{\frac{1}{2}}\|\mathcal{P}_\partial p_\epsilon - \lambda_h^{os}\|_{0,e}. \tag{A.4}$$

Define $\tau_h = \tilde{\tau}_h$ in K and $\tau_h = 0$ in $\Omega\backslash$ K. By the second equation in (3.11), we have

$$(\theta_h^{os}, \tilde{\tau}_h)_K + (p_h^{os}, div\tilde{\tau}_h)_K = (\mathcal{P}_\partial p_\epsilon - \lambda_h^{os}, \lambda_h^{os})_e.$$

Since $div\mathcal{M}_h(\tilde{\tau}_h) = div\tilde{\tau}_h$, it follows that

$$(\theta_h^{os}, \tilde{\tau}_h)_K + (p_h^{os}, div\mathcal{M}_h(\tilde{\tau}_h))_K = (\mathcal{P}_\partial p_\epsilon - \lambda_h^{os}, \lambda_h^{os})_e. \tag{A.5}$$

Since $\theta_\epsilon = \nabla p_\epsilon$, Green's function gives

$$(\theta_\epsilon, \mathcal{M}_h(\tilde{\tau}_h))_K + (p_\epsilon, div\mathcal{M}_h(\tilde{\tau}_h))_K = (\mathcal{P}_\partial p_\epsilon - \lambda_h^{os}, p_\epsilon)_e. \tag{A.6}$$

By a similar argument to (4.6), it follows that

$$\|v_h\|_{0,K} \le C\|\mathcal{M}_h v_h\|_{0,K} \quad \text{for} \quad \forall v_h \in \tilde{X}_{2,h}^{os}(K). \tag{A.7}$$

By using (A.5), (A.6), (A.4) and (A.7), we get

$$\begin{aligned}
&\|\mathcal{P}_\partial p_\epsilon - \lambda_h^{os}\|_{0,e}^2 = (\mathcal{P}_\partial p_\epsilon - \lambda_h^{os}, \mathcal{P}_\partial p_\epsilon - \lambda_h^{os})_e = (p_\epsilon - \lambda_h^{os}, \mathcal{P}_\partial p_\epsilon - \lambda_h^{os})_e \\
&= (\theta_\epsilon - \theta_h^{os}, \tilde{\tau}_h)_K + (\theta_\epsilon, \mathcal{M}_h(\tilde{\tau}_h) - \tilde{\tau}_h)_K + (p_\epsilon - p_h^{os}, div\mathcal{M}_h(\tilde{\tau}_h))_K \\
&\le \|\theta_\epsilon - \theta_h^{os}\|_{0,K}\|\tilde{\tau}_h\|_{0,K} + \|\theta_\epsilon\|_{0,K}(\|\mathcal{M}_h(\tilde{\tau}_h)\|_{0,K} + \|\tilde{\tau}_h\|_{0,K}) \\
&+ \|p_\epsilon - p_h^{os}\|_{0,K}\|div\mathcal{M}_h(\tilde{\tau}_h)\|_{0,K} \\
&\le C\|\theta_\epsilon - \theta_h^{os}\|_{0,K}\|\mathcal{M}_h(\tilde{\tau}_h)\|_{0,K} + C\|\theta_\epsilon\|_{0,K}\|\mathcal{M}_h(\tilde{\tau}_h)\|_{0,K} + \|p_\epsilon - p_h^{os}\|_{0,K}\|div\mathcal{M}_h(\tilde{\tau}_h)\|_{0,K} \\
&\le C\big(h_K^{-\frac{1}{2}}\|p_\epsilon - p_h^{os}\|_{0,K} + h_K^{\frac{1}{2}}\|\theta_\epsilon - \theta_h^{os}\|_{0,K} + h_K^{\frac{1}{2}}\|\theta_\epsilon\|_{0,K}\big)\|\mathcal{P}_\partial p_\epsilon - \lambda_h^{os}\|_{0,e},
\end{aligned} \tag{A.8}$$

which gives

$$\|\mathcal{P}_\partial p_\epsilon - \lambda_h^{os}\|_{0,e} \le C\big(h_K^{-\frac{1}{2}}\|p_\epsilon - p_h^{os}\|_{0,K} + h_K^{\frac{1}{2}}\|\theta_\epsilon - \theta_h^{os}\|_{0,K} + h_K^{\frac{1}{2}}\|\theta_\epsilon\|_{0,K}\big).$$

Consequently,

$$\begin{aligned}
\|\mathcal{P}_\partial p_\epsilon - \lambda_h^{os}\|_{-\frac{1}{2},h}^2 &= \sum_{K\in\mathfrak{T}_h}\sum_{e\in\subset\partial K} h_K\|\mathcal{P}_\partial p_\epsilon - \lambda_h^{os}\|_{0,e}^2 \\
&\le C\|p_\epsilon - p_h^{os}\|_{0,\Omega}^2 + Ch^2\|\theta_\epsilon - \theta_h^{os}\|_{0,\Omega}^2 + Ch^2\|\theta_\epsilon\|_{0,K}.
\end{aligned} \tag{A.9}$$

Combining (A.1), (A.2), (A.3) and (A.9) proves (4.41).

Appendix B. proof of Theorem 4.18.

By straightforward calculation, it follows that

$$\begin{cases} div[\sum_{i=1}^N \sum_{e\subset\partial K}(\int_e A_i u_i\cdot n_e ds)(-k\nabla\phi_{i,\chi_e}^K)] & = div(\mathcal{I}_h^g u|_K) \quad \text{in } K \\ \sum_{i=1}^N \sum_{e\subset\partial K}(\int_e A_i u_i\cdot n_e ds)(-k\nabla\phi_{i,\chi_e}^K)\cdot n & = (\mathcal{I}_h^g u|_K)\cdot n \quad \text{on} \quad \partial K. \end{cases} \tag{B.1}$$

Comparing equation (4.51) with equation (B.1), we find that

$$-k\nabla w = \sum_{i=1}^{N}\sum_{e\subset\partial K}(\int_e A_i u_i\cdot n_e ds)(-k\nabla\phi_{i,\chi_e}^K) = \mathcal{I}_h^g u|_K.$$

By the uniqueness of solution for (4.51), it follows that

$$\nabla w = \sum_{i=1}^{N}\sum_{e\subset\partial K}(\int_e A_i u_i\cdot n_e ds)\eta_{i,\chi_e}^K \in X_{1,h}^g(K).$$

REFERENCES

[1] J. E. Aarnes, Y. Efendiev and L. Jiang, *Mixed multiscale finite element methods using limited global information*, Multiscale Modeling and Simulation, 7 (2008), pp. 655–676.

[2] J. Aarnes, S. Krogstad, K. A. Lie, A hierarchical multiscale method for two-phase flow based on upon mixed finite elements and nonuniform coarse grids, Multiscale Modeling and Simulation, 5 (2006), pp. 337-363.

[3] G. Allaire and R. Brizzi, A multiscale finite element method for numerical homogenization, Multiscale Modeling and Simulation, 4 (2005), pp. 790–812.

[4] T. Arbogast, *Implementation of a locally conservative numerical subgrid upscaling scheme for two-phase Darcy flow*, Comput. Geosci., 6 (2002), pp. 453–481.

[5] T. Arbogast and K. J. Boyd, *Subgrid upscaling and mixed multiscale finite elements*, SIAM J. Numer. Anal., 44 (2006), pp. 1150-1171.

[6] T. Arbogast, G. Pencheva, M. F. Wheeler, and I. Yotov, *A multiscale mortar mixed finite element method*, Multiscale Modeling and Simulation, 6 (2007), pp. 319-346.

[7] T. Arbogast, M. F. Wheeler and I. Yotov, *Mixed finite elments for elliptic problems with tensor coefficients as cell-centered finite differences*, SIAM J. Numer. Anal., 34 (1997), pp. 828–852.

[8] D. N. Arnold and F. Brezzi, *Mixed and nonconforming finite element method: implementation, postprocessing and error estimates*, Math. Modelling and Numer. Anal., 19 (1985), pp. 7–35.

[9] I. Babuška and E. Osborn, *Generalized finite element methods: Their performance and their relation to mixed methods*, SIAM J. Numer. Anal., 20 (1983), pp. 510–536.

[10] L. Berlyand and H. Owhadi, *Flux norm approach to finite dimensional homogenization approximations with non-separated scales and high contrast*, Archives for Rational Mechanics and Analysis, 198 (2010), pp. 677-721.

[11] F. Brezzi, *Interacting with the subgrid world*, in Numerical analysis 1999 (Dundee), Chapman & Hall/CRC, Boca Raton, FL, 2000, pp. 69–82.

[12] F. Brezzi and M. Fortin, *Mixed and hybrid finite element methods*, 1991, Springer–Verlag, New York.

[13] Z. Chen, *Expanded mixed finite element methods for quasilinear second-order elliptic problems*, Math. Modelling Numer. Anal. 32 (1998), pp. 501–520.

[14] Z. Chen and T. Y. Hou, *A mixed multiscale finite element method for elliptic problems with oscillating coefficients*, Math. Comp., 72 (2002), pp. 541–576.

[15] C. C. Chu, I. G. Graham and T. Y. Hou, *A new multiscale finite element method for high-contrast elliptic interface problems*, Math. Comp. 79 (2010), pp. 1915-1955.

[16] E. T. Chung and Y. Efendiev, *Reduced-contrast approximations for high-contrast multiscale flow problems*, Multiscale Modeling and Simulation, 8 (2010), pp. 1128-1153.

[17] W. E and B. Engquist, *The heterogeneous multi-scale methods*, Comm. Math. Sci., 1 (2003), pp. 87–133.

[18] Y. Efendiev, J. Galvis and X. Wu, *Multiscale finite element methods for high-contrast problems using local spectral basis functions*, J. Comput. Phys., 230 (2011), pp. 937-955.

[19] B. M. Fraejis De Veubeke, *Displacement and equilibrium models in the finite element method*, in Stree Aanalysis, O. Zienkiewicz and G. Holister, eds., Wiley, New York, 1977, pp. 145–197.

[20] G. N. Gatica, *Solvability and Galerkin approximations of a class of nonlinear operator equations*, Z. Anal. Anwendungen 21 (2002), pp. 761–781.

[21] G. N. Gatica and N. Heuer, *An expanded mixed finite element approach via a dual dual formulation and the minimum residual method*, Journal of Compuatational and Applied Mathematics, 132 (2001), pp. 371–385.

[22] A. Gloria, *Reduction of the resonance error. Part 1: Approximation of homogenized coefficients*, M3AS, 21 (2011), pp. 1601–1630.

[23] T. Y. Hou and X. H. Wu, *A multiscale finite element method for elliptic problems in composite materials and porous media*, J. Comput. Phys., 134 (1997), pp. 169–189.

[24] T. Hughes, G. Feijoo, L. Mazzei, and J. Quincy, *The variational multiscale method - a paradigm for computational mechanics*, Comput. Methods Appl. Mech. Engrg, 166 (1998), pp. 3–24.

[25] P. Jenny, S. H. Lee, and H. Tchelepi, *Multi-scale finite volume method for elliptic problems in subsurface flow simulation*, J. Comput. Phys., 187 (2003), pp. 47–67.

[26] L. Jiang, Y. Efendiev and I. Mishev, *Mixed multiscale finite element methods using approximate global information based on partial upscaling*, Comput. Geosci., 14 (2010), pp. 319–341.

[27] V. Jikov, S. Kozlov, and O. Oleinik, *Homogenization of differential operators and integral functionals,* Springer-Verlag, 1994, Translated from Russian.

[28] K. Lipnikov, J. D. Moulton and D. Svyatskiy, *A multilevel multiscale mimetic (M^3) method for two-phase flows in porous media*, J. Comput. Phys., 227 (2008), pp. 6727–6753.

[29] F. Murat and L. Tartar, *H-convergence, in topics in the mathematical modeling of composite materials, A. Cherkaev and R.V. Kohn eds.series: Progress in Nonlinear Differential equations and their Applications*, Birkhauser, Boston 1997.

[30] H. Owhadi and L. Zhang, *Metric based up-scaling*, Com. Pure Appl. Math., 60 (2007), pp. 675-723

[31] D. W. Peaceman, *Interpretation of well-block pressures in numerical reservoir simulation*, Soc. Petro. Engrg. J. (1978), pp. 183–194.

[32] C. S. Woodward and C. N. Dawson, *Analysis of expanded mixed finite element methods for a nonlinear parabolic equation modeling flow into variably saturated porous media*, SIAM J. Numer. Anal., 37 (2000), pp. 701–724.